Black holes and Gravitational waves

Lecture 4

Konstantin Postnov
SAI MSU
Faculty of Physics, MSU

Plan

- Basic GW: GR
- Principle of detection: GW interferometers
- Astrophysical sources
- GW from compact binaries
- GW astronomy: first results and prospects

Nobel Prize in physics 2017

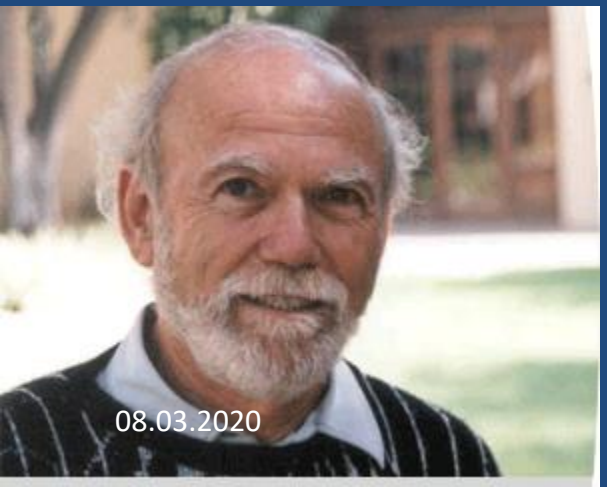

Very brief history

- 1916, A. Einstein
- 1920s (Einstein, Eddington, …)
- 1962, M.E. Gertsenstein & V.I. Pustovoit – laser interferometers as GW detectors
- 1970s, R&D (R. Weiss, R. Drever, K. Thorne, V. Braginskii …)
- End of the 1980s: start of LIGO project
- 2002-2010, initial LIGO operation
- 2010-2015, LIGO modernization
- September 14, 2015, first detection of binary BH coalescence (GW 150914)
- August 17, 2017, first detection of binary NS coalescence (GW 170817), start of multmessenger astronomy

Main results 2015-2020

- 10 reliably detected BH+BH with M=10-50 $M_\odot$ from distances 500-1000 Mpc
- Merging rate ~12-213 Gpc^{-3} yr^{-1}
- Measured properties consistent with GR up to a few %
- One reliable NS+NS merging (GW170817) and observations of gamma-ray to radio afterglow from relativistic jet and kilonova

General Relativity

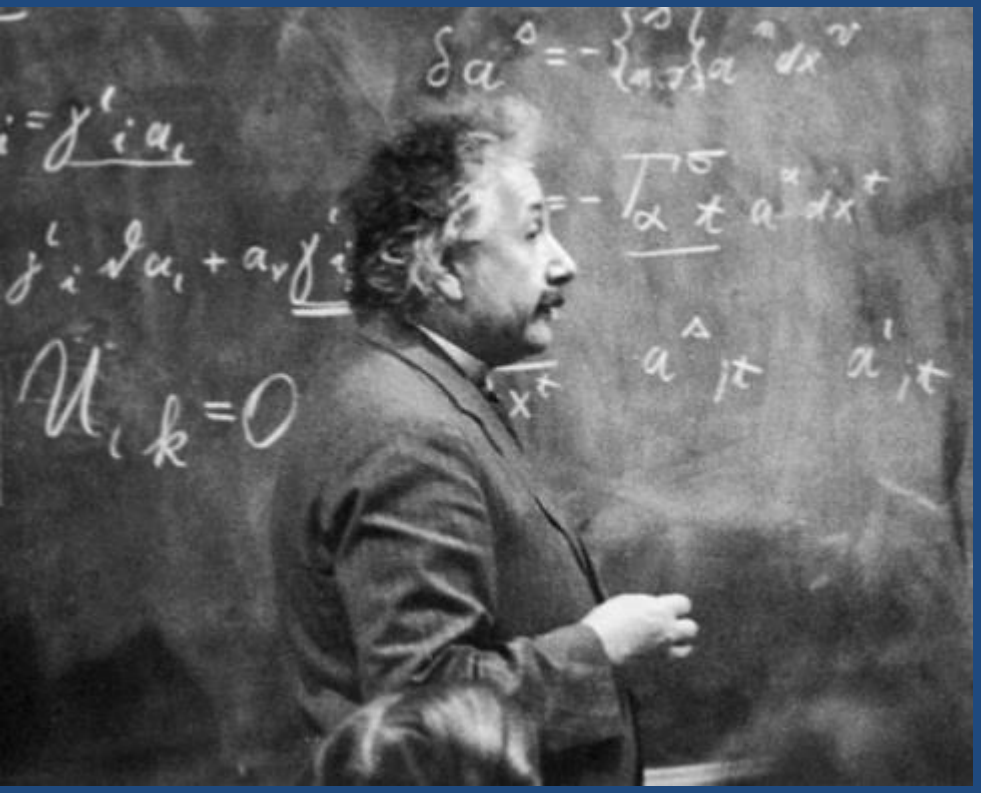

- A. Einstein, 1915
- Gravitation = curvature of space-time

$$R_{\mu\nu} - \frac{1}{2} R g_{\mu\nu} = \frac{8\pi G}{c^4} T_{\mu\nu}, \qquad ds^2 = g_{\mu\nu} dx^\mu dx^\nu$$

GW as a «ripple» of space-time

$$g_{\alpha\beta} = g^{\mathrm{B}}_{\alpha\beta} + h_{\alpha\beta}\ , \qquad R_{\alpha\beta\gamma\delta} = R^{\mathrm{B}}_{\alpha\beta\gamma\delta}$$

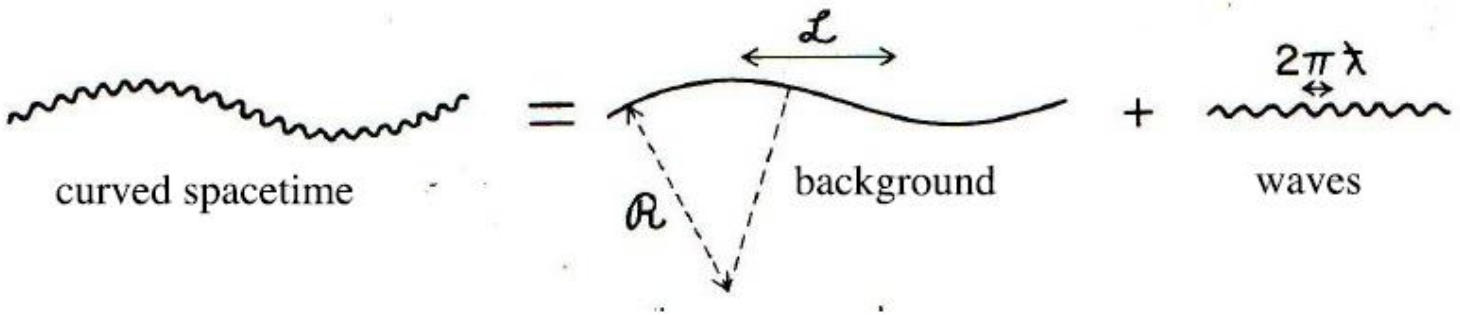

Linearized gravity

$$g_{\mu\nu} = \eta_{\mu\nu} + h_{\mu\nu}, \quad |h_{\mu\nu}| \ll 1.$$

$$x^\mu \longrightarrow x'^\mu = x^\mu + \xi^\mu(x)$$

$$h_{\mu\nu}(x) \longrightarrow h'_{\mu\nu}(x') = h_{\mu\nu}(x) - (\partial_\mu \xi_\nu + \partial_\nu \xi_\mu)$$

$$R_{\mu\nu\rho\sigma} = \frac{1}{2}(\partial_\nu\partial_\rho h_{\mu\sigma} + \partial_\mu\partial_\sigma h_{\nu\rho} - \partial_\mu\partial_\rho h_{\nu\sigma} - \partial_\nu\partial_\sigma h_{\mu\rho})$$

Gauge-invariant!!!

$$\bar{h}_{\mu\nu} = h_{\mu\nu} - \frac{1}{2}\eta_{\mu\nu}h,$$

$$\bar{h}_{\mu\nu} \longrightarrow \bar{h}'_{\mu\nu} = \bar{h}_{\mu\nu} - (\partial_\mu \xi_\nu + \partial_\nu \xi_\mu - \eta_{\mu\nu}\partial_\rho \xi^\rho)$$

$$\Box \bar{h}_{\mu\nu} = -\frac{16\pi G}{c^4} T_{\mu\nu}$$

$$\partial^\nu \bar{h}_{\mu\nu} = 0.$$

$$\partial^\nu T_{\mu\nu} = 0$$

Gravitational waves

$$c^2\bar{h}^{00} = -4\phi \qquad c^2 h_{00} = -2\phi \qquad \Delta\phi = 4\pi G\rho$$

- Convenient gauge

$$\Box\xi_\mu = 0.$$

$$\xi_{\mu\nu} = \partial_\mu\xi_\nu + \partial_\nu\xi_\mu - \eta_{\mu\nu}\partial_\rho\xi^\rho \qquad \Box\xi_{\mu\nu} = 0$$

- Does not change linearized equations and harmonic (Lorentz) gauge $\partial^\nu\bar{h}_{\mu\nu} = 0.$
- **4 arbitrary functions ξ can be used to vanish 4 components to leave only 2 independent components (polarizations)**

TT-gauge (transverse-traceless)

$$1)\,\textit{Vanish trace}: \xi_0(x): \bar{h} = 0 \Rightarrow \bar{h}_{\mu\nu} = h_{\mu\nu}$$

$$2)\,\textit{Make transverse}: \xi_i(x): h_{0\mu} = 0: \quad \partial^i h_{ij} = 0$$

$$h_{0\mu} = 0, \quad h^i{}_i = 0, \quad \partial^j h_{ij} = 0$$

$$h_{ij}^{\mathrm{TT}} = e_{ij}(\mathbf{k})\,\cos(k_\mu x^\mu)$$

$$k_\mu = (\omega/c, \mathbf{k}) \qquad \omega = c|\mathbf{k}|$$

$$\partial^j h_{ij} = 0 \quad \Rightarrow \quad \mathbf{k}^j h_{ij}^{\mathrm{TT}} = 0 \qquad n^j h_{ij}^{\mathrm{TT}} = 0 \qquad \hat{\mathbf{n}} = \mathbf{k}/|\mathbf{k}|$$

$$h_{ij}^{\mathrm{TT}} = \begin{pmatrix} h_+ & h_\times & 0 \\ h_\times & -h_+ & 0 \\ 0 & 0 & 0 \end{pmatrix}_{ij} \cos\left[\omega(t - z/c)\right]$$

Transition to TT-gauge

$$h_{\alpha\beta} = h_{\alpha\beta}(t - \mathbf{n}\cdot\mathbf{x}) \qquad \bar{h}_{\alpha\beta} = \bar{h}_{\alpha\beta}(t - \mathbf{n}\cdot\mathbf{x})$$

$$P^{jk} \equiv \delta^{jk} - n^j\, n^k$$

$$h^{\mathrm{TT}}_{jk} = (\bar{h}_{jk})^{\mathrm{TT}} = P_j{}^l P_k{}^m \bar{h}_{lm} - \frac{1}{2} P_{jk} P^{lm} \bar{h}_{lm}$$

- For example. For a wave moving along z-axis:

$$h_+ = h^{\mathrm{TT}}_{xx} = \bar{h}_{xx} - \frac{1}{2}(\bar{h}_{xx} + \bar{h}_{yy}) = \frac{1}{2}(h_{xx} - h_{yy})\,, \quad h_\times = h^{\mathrm{TT}}_{xy} = \bar{h}_{xy}$$

TT-GW acting on two test masses

$$\frac{d^2x^\mu}{d\tau^2} + \Gamma^\mu_{\nu\rho}(x)\frac{dx^\nu}{d\tau}\frac{dx^\rho}{d\tau} = 0.$$

$$\frac{d^2(x^\mu+\zeta^\mu)}{d\tau^2} + \Gamma^\mu_{\nu\rho}(x+\zeta)\frac{d(x^\nu+\zeta^\nu)}{d\tau}\frac{d(x^\rho+\zeta^\rho)}{d\tau} = 0$$

$$\frac{d^2\zeta^\mu}{d\tau^2} + 2\Gamma^\mu_{\nu\rho}\frac{dx^\nu}{d\tau}\frac{d\zeta^\rho}{d\tau} + \zeta^\sigma\partial_\sigma\Gamma^\mu_{\nu\rho}(x)\frac{dx^\nu}{d\tau}\frac{dx^\rho}{d\tau} = 0.$$

$$\frac{DV^\mu}{D\tau} = \frac{dV^\mu}{d\tau} + \Gamma^\mu_{\nu\rho}V^\nu\frac{dx^\rho}{d\tau}$$

$$\frac{D^2\zeta^\mu}{D\tau^2} = -R^\mu{}_{\nu\rho\sigma}\zeta^\rho\frac{dx^\nu}{d\tau}\frac{dx^\sigma}{d\tau}$$

- In local Lorentz frame :

$$\Gamma^{\mu}_{\nu\rho}(P) = 0.$$

$$\frac{d^2\zeta^i}{d\tau^2} = -R^i{}_{0j0}\zeta^j \left(\frac{dx^0}{d\tau}\right)^2$$

- Non-relativistic motion of masses:

$$dx^0/d\tau \simeq c$$

$$\ddot{\zeta}^i = -c^2 R^i{}_{0j0}\zeta^j \qquad R^i{}_{0j0} = R_{i0j0} = -\frac{1}{c^2}\ddot{h}^{\rm TT}_{ij}$$

$$R_{\alpha\beta\gamma\delta} = \frac{1}{2}h^{\rm TT}_{\{\alpha\beta,\gamma\delta\}} \equiv \frac{1}{2}(h^{\rm TT}_{\alpha\delta,\beta\gamma} + h^{\rm TT}_{\beta\gamma,\alpha\delta} - h^{\rm TT}_{\alpha\gamma,\beta\delta} - h^{\rm TT}_{\beta\delta,\alpha\gamma})$$

$$\ddot{\zeta}^i = \frac{1}{2}\ddot{h}^{\rm TT}_{ij}\zeta^j.$$

$$\delta x^j = \frac{1}{2}h^{\rm TT}_{jk}x^k$$

Simple argument by R.Feynmann (1957, Chapel Hill conference)

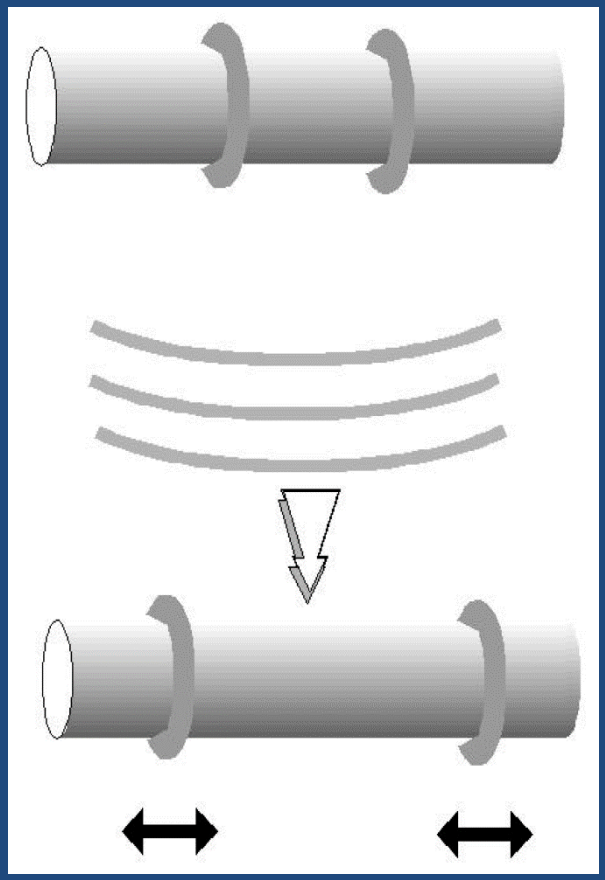

- “I was surprised to find that a whole day of the conference was spent on this issue and that ‘experts’ were confused. That’s what happens when one is considering energy conservation tensors, etc. instead of questioning, can waves do work?”

(after F. Pirani’s talk)

Energy flux in GW

- Energy density

$$t^{00} = \frac{c^2}{16\pi G}\langle \dot{h}_+^2 + \dot{h}_\times^2 \rangle$$

- Energy flux

$$\frac{dE_{\rm GW}}{dt} = \frac{c^3 r^2}{16\pi G}\int d\Omega \, \langle \dot{h}_+^2 + \dot{h}_\times \rangle .$$

- GW carries energy and momentum that can act on test masses

$$T^{{\rm GW}\,0z} \simeq \frac{\pi}{4}\frac{c^3}{G} f^2 h_{\rm amp}^2 \simeq 300 \frac{\rm ergs}{\rm cm^2\ sec}\left(\frac{f}{1\ {\rm kHz}}\right)^2\left(\frac{h_{\rm amp}}{10^{-21}}\right)^2$$

GW sources

$$\bar{h}_{\mu\nu}(t,\mathbf{x}) = -4\frac{G}{c^2}\int_{\mathcal{V}} \frac{T_{\mu\nu}(t-|\mathbf{x}-\mathbf{x}'|/c,\mathbf{x}')}{|\mathbf{x}-\mathbf{x}'|}d^3\mathbf{x}'$$

- Lowes order -- quadrupole. For v/c<<1:

$$h_{jk}^{\mathrm{GW}} = 2G\frac{\ddot{I}_{jk}}{r} \sim G\frac{\omega^2(ML^2)}{r} \sim G\frac{E_{\mathrm{kin}}/c^2}{r}$$

$$h_{jk}^{\mathrm{GW}} \sim h_+ \sim h_\times \sim 10^{-21}\left(\frac{E_{\mathrm{kin}}}{M_\odot c^2}\right)\left(\frac{100\mathrm{Mpc}}{r}\right)$$

GE creates tidal acceleration field in a freely faling (local Lorentz) reference frame

$$\mathcal{E}_{ij} = R_{i0j0} = -\frac{1}{2}\ddot{h}_{ij}^{\mathrm{TT}}$$

$$h_{ij}^{\mathrm{TT}} \equiv -2\int dt \int dt\, \mathcal{E}_{ij}$$

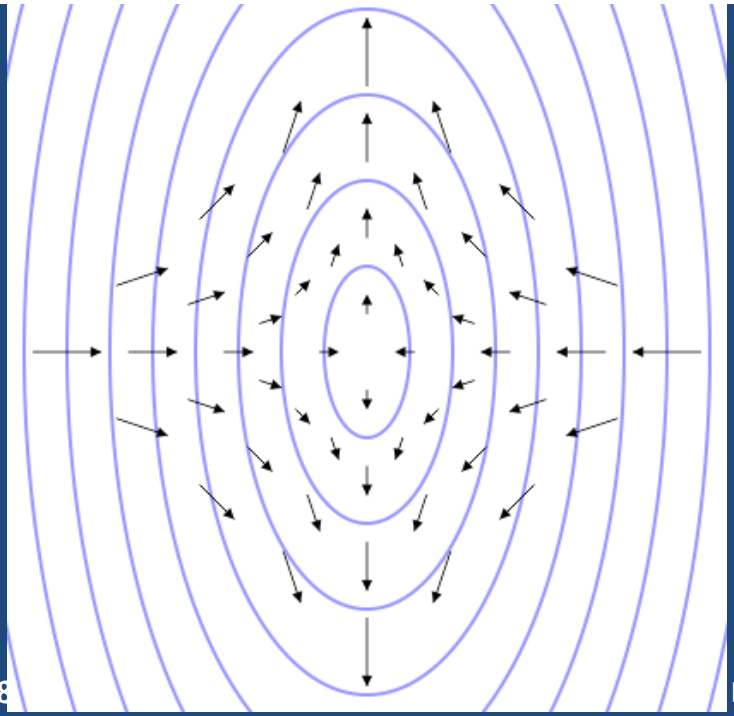

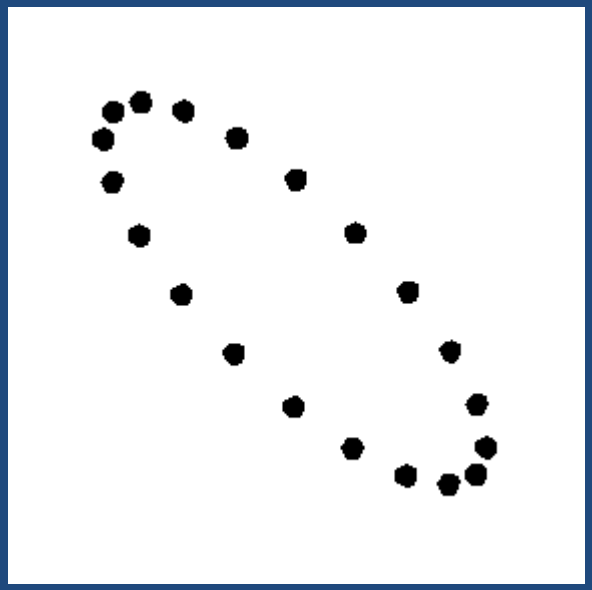

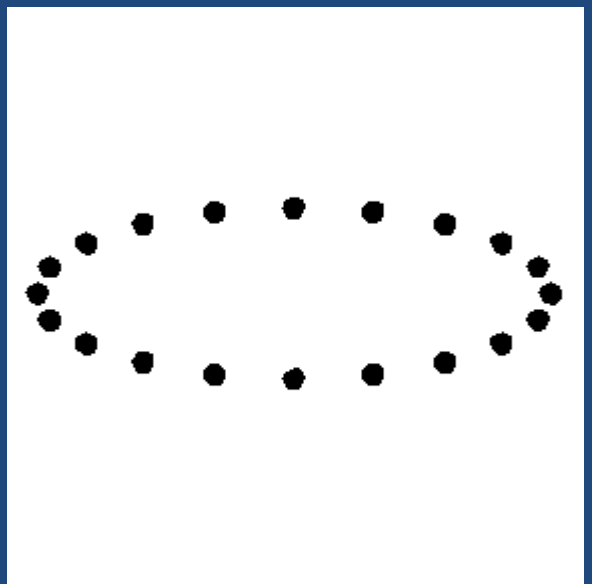

GW amplitude h = relative expansion/compression

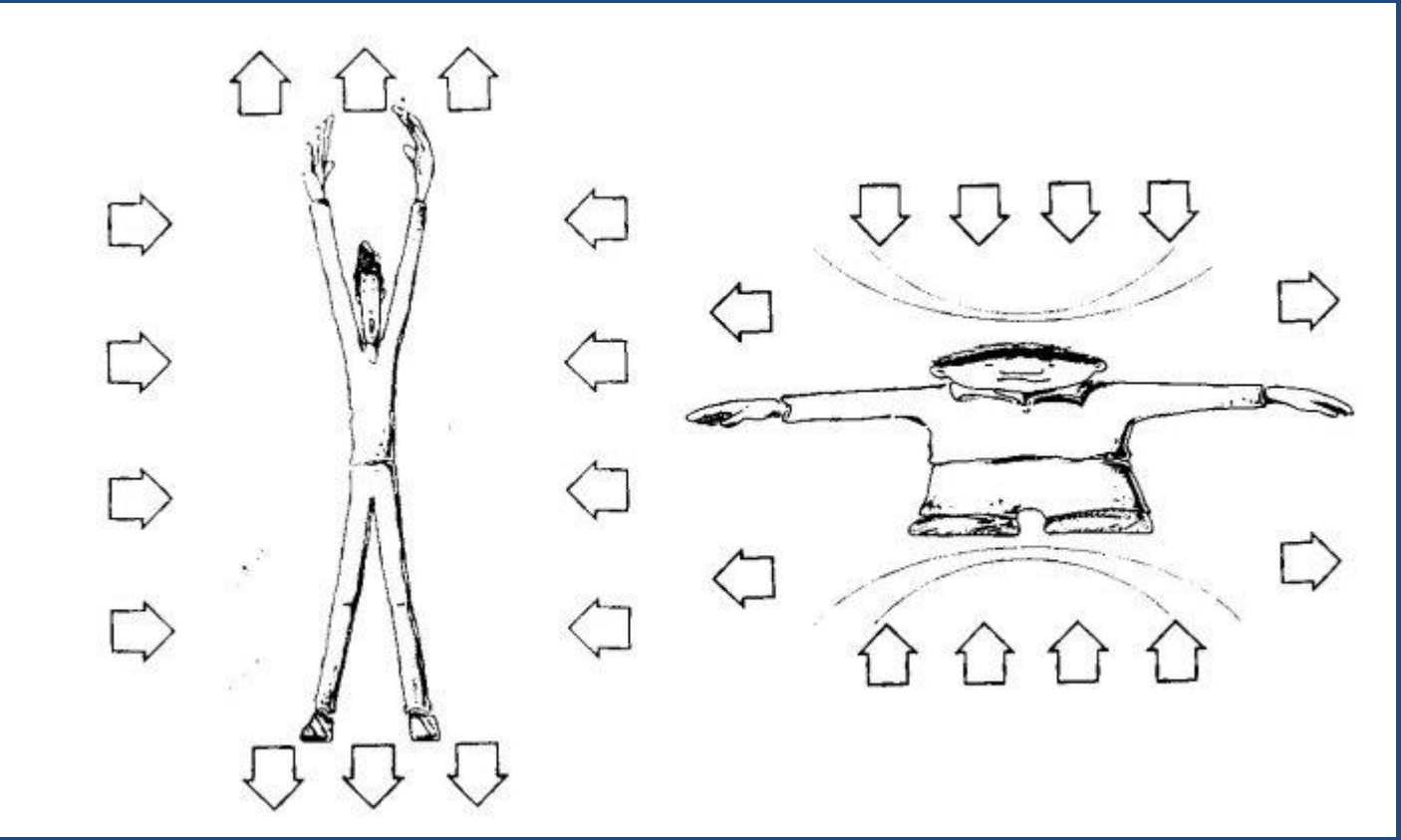

Tidal acceleration field

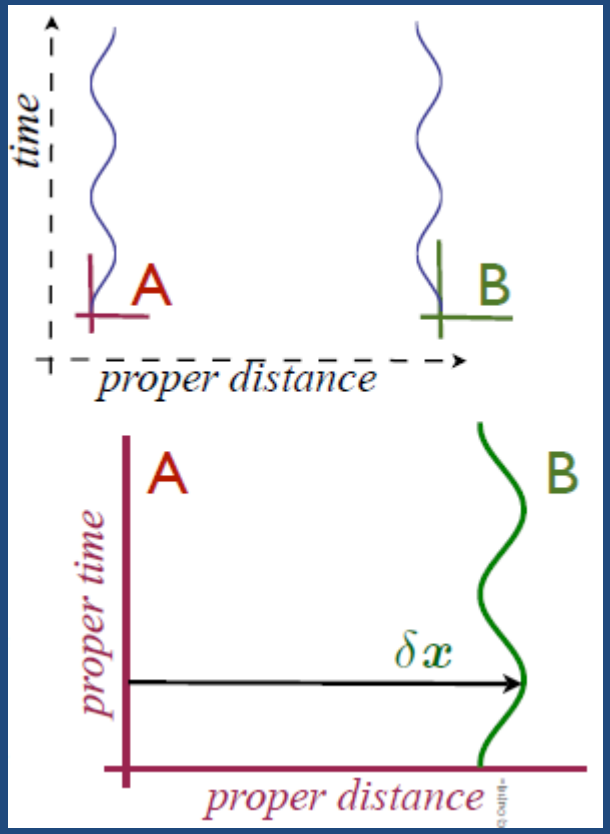

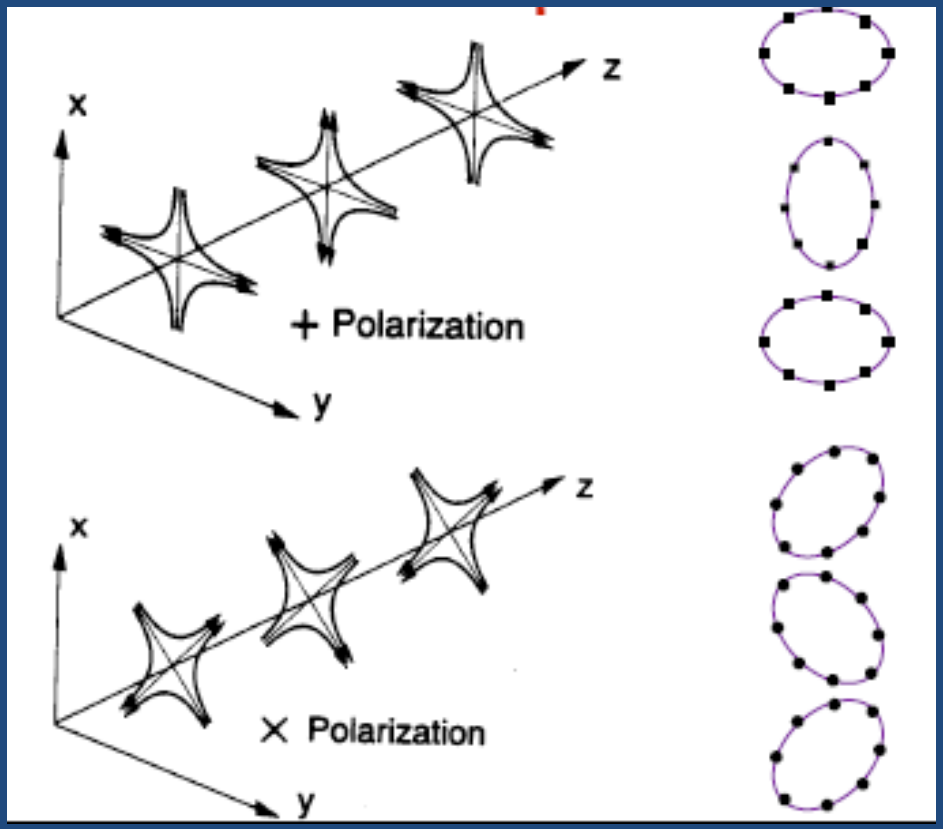

$$\delta x_j = \frac{1}{2} h_{jk}^{\mathrm{GW}} x_k$$

Astrophysical GW sources

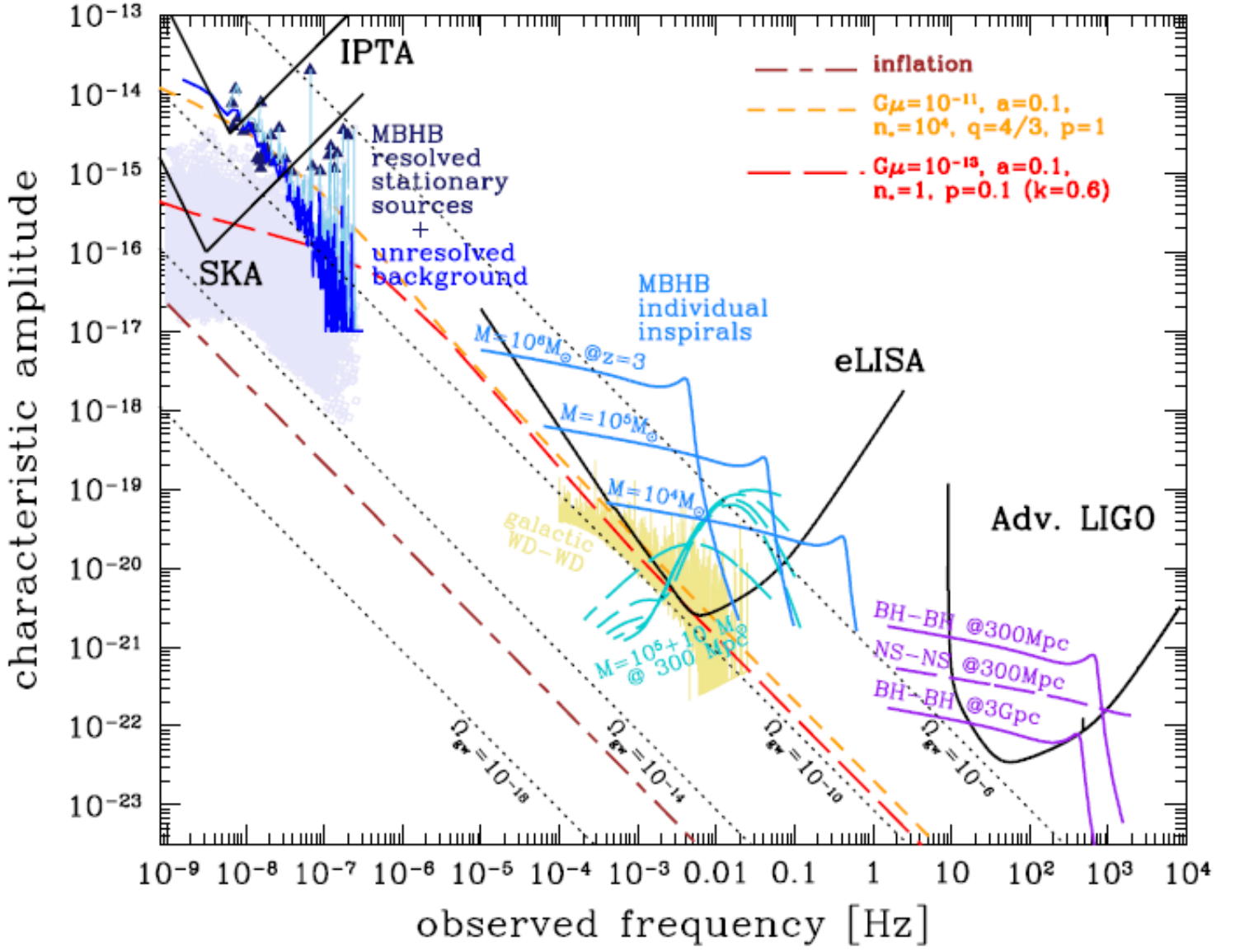

Credit: A. Sesana

Coalescing compact binaries

E pur si existare!

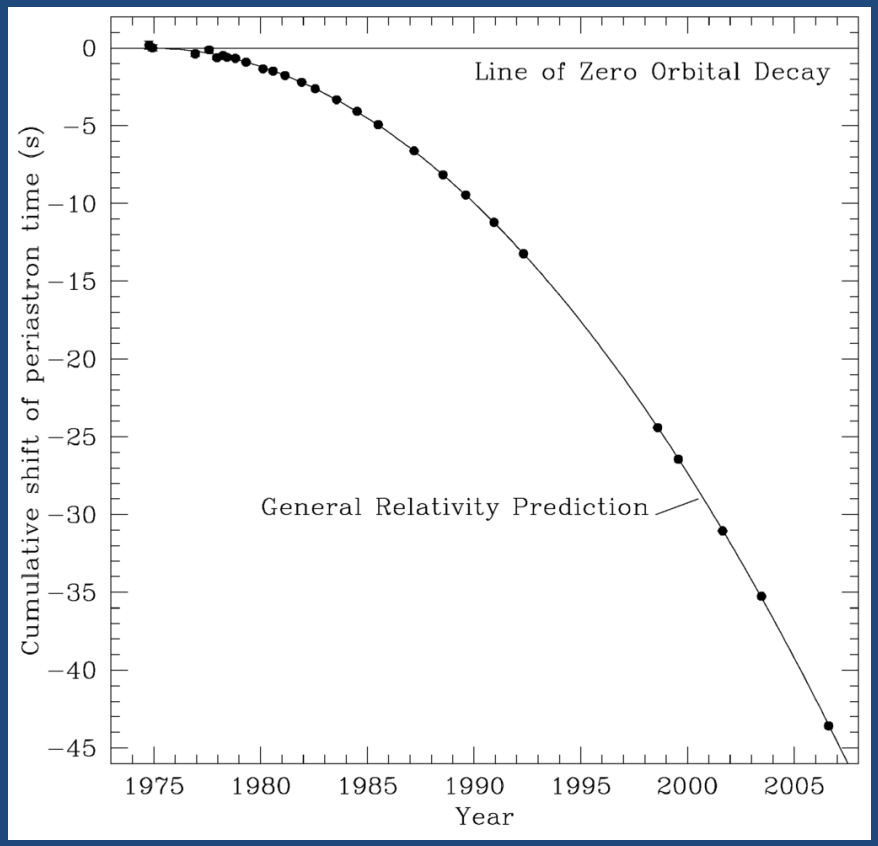

- 1974, binary pulsar PSR 1913+16 (Hulse, Taylor, Nobel Prize 1993)

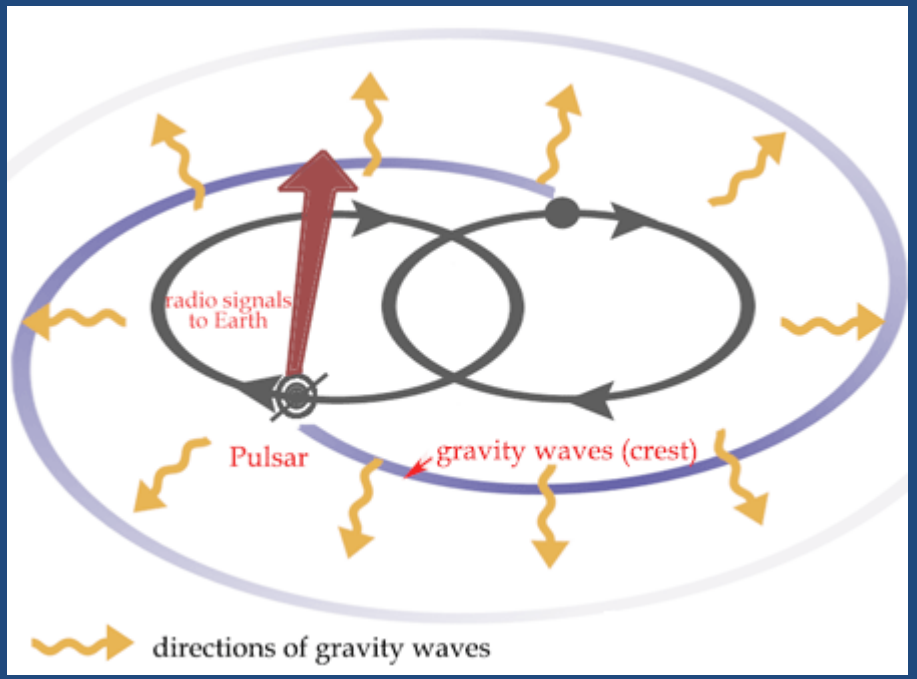

Orbital period decay in agreement with GR (~0.1%)

EM vs GW

	EM	GW
Charge	q	m
Size	R	$\omega^2 \sim \frac{m}{R^3}[G]$
Dipole radiation	$A \sim \frac{qR\omega}{r}$	no
Quadrupole radiation	Dipole x (v/c)	$h \sim \frac{mR^2\omega^2}{r}\left[\frac{G}{c^4}\right]$
Energy flux	$F_{EM} \sim \omega^2 A^2 \sim \frac{q^2 \ddot{R}^2}{r^2}$	$F_{GW} \sim \omega^2 h^2 \sim \frac{m^2 R^4 \omega^6}{r^2}\left[\frac{G}{c^4}\right]^2$
Power	$\frac{dE}{dt} = -\frac{2}{3}\ddot{d}^2$	$\frac{dE}{dt} = -\frac{128}{5} m^2 R^4 \omega^6 \left[\frac{G}{c^5}\right]$

- Waveform from two coalescing point-like masses is determined by a combination of component masses (the chirp mass)
- ➔ blackboard

$$M_{ch} = (\mu^3 M^2)^{1/5}$$

$$h \sim M_{ch}^{5/3} f^{2/3} / r$$

$$\mathcal{M} = \frac{(m_1 m_2)^{3/5}}{(m_1 + m_2)^{1/5}} = \frac{c^3}{G}\left(\frac{5}{96}\pi^{-8/3} f^{-11/3} \dot{f}\right)^{3/5}$$

Chirp signal from a coalescing binary

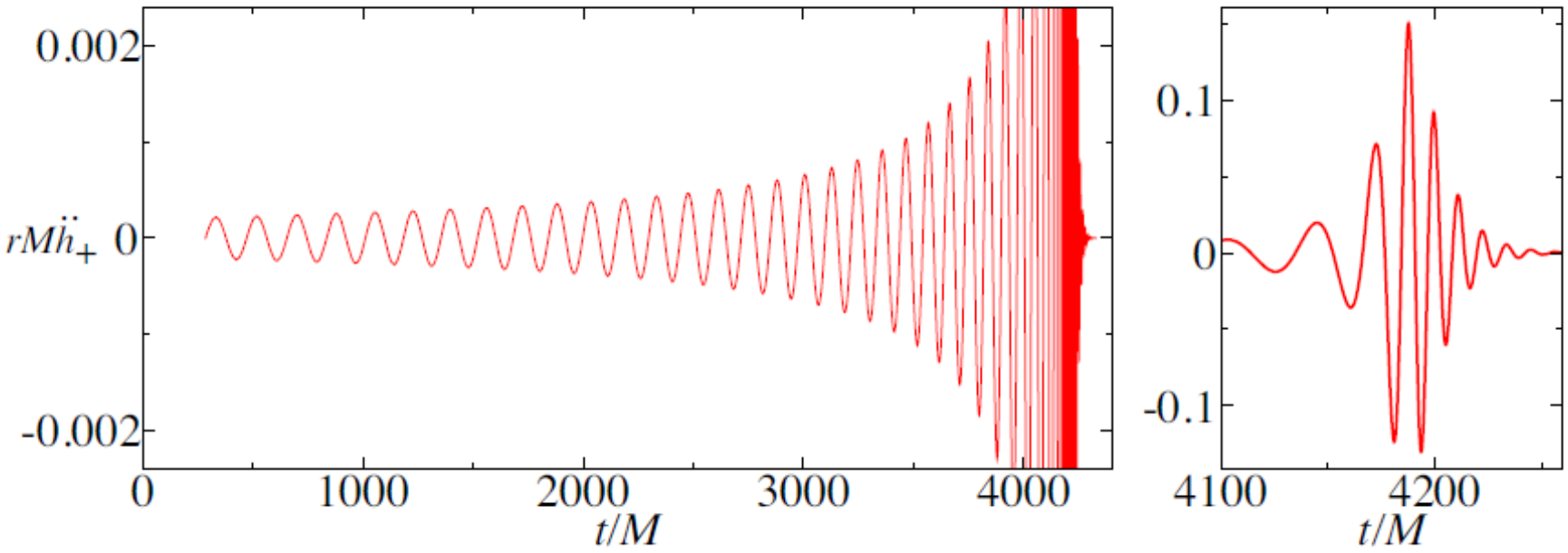

$$h_+ = h^{\rm TT}_{\hat\theta\hat\theta} = \frac{2}{r}[\ddot I_{\hat\theta\hat\theta}(t-r)]^{\rm TT} = -2(1+\cos^2\theta)\,\frac{\mu(M\Omega)^{2/3}}{r}\cos[2(\Omega t - \Omega r - \phi)]$$

$$h_\times = h^{\rm TT}_{\hat\theta\hat\phi} = \frac{2}{r}[\ddot I_{\hat\theta\hat\phi}(t-r)]^{\rm TT} = -4\cos\theta\,\frac{\mu(M\Omega)^{2/3}}{r}\sin[2(\Omega t - \Omega r - \phi)]\,.$$

Signal from binary rotating BHs is much more complicated

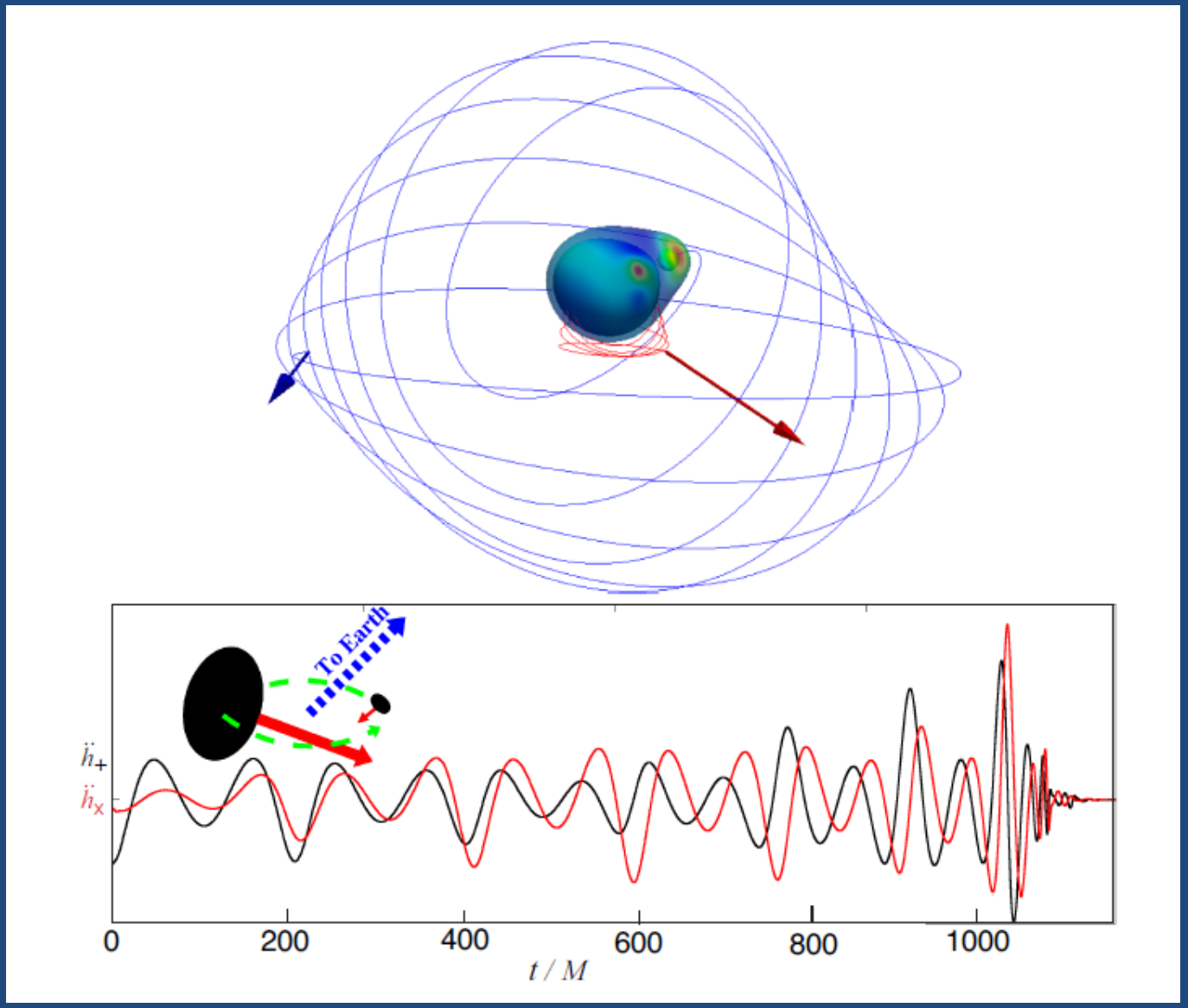

Energy release in binary BH mergings

$$E_N = (m_1 + m_2)c^2 - \frac{Gm_1m_2}{2r}$$

$$r_{insp} \approx \frac{5G(m_1 + m_2)}{c^2} \quad \Rightarrow$$

$$\Delta E_{GW,insp} \approx \frac{1}{10}\frac{m_1m_2}{m_1 + m_2} \approx 5\% mc^2 \sim 2.5\% Mc^2$$

$$\Delta E_{GW,total} = \Delta E_{GW,insp} + \Delta E_{GW,coal} + \Delta E_{GW,ringd} \approx 5\% Mc^2$$

$$\Delta E_{GW,total} = (M_i^{source} - M_f^{source})c^2 = 3^{+0.5}_{-0.5} M_\odot c^2$$

Maximum luminosity

$$\frac{dE}{dtdA} = \frac{c^3}{16\pi G}\left(\left\langle \dot{h}_{\times} \right\rangle^2 + \left\langle \dot{h}_{\times} \right\rangle^2\right)$$

$$h_{\max} \sim 10^{-21}, d \sim 400\,Mpc \quad \Rightarrow$$

$$\left(\frac{dE}{dt}\right)_{GW,\max} \sim 10^{56}\,erg/s \sim 200 M_{\odot} c^2/s$$

$$\left(\frac{dE}{dt}\right)_{GW,\max} \le L_0 = \frac{c^5}{16\pi G} \approx 7\times 10^{57}\,erg/s$$

$$(Cf\ \ the\ brightest\ GRB: 2\times 10^{54}\,erg/s)$$

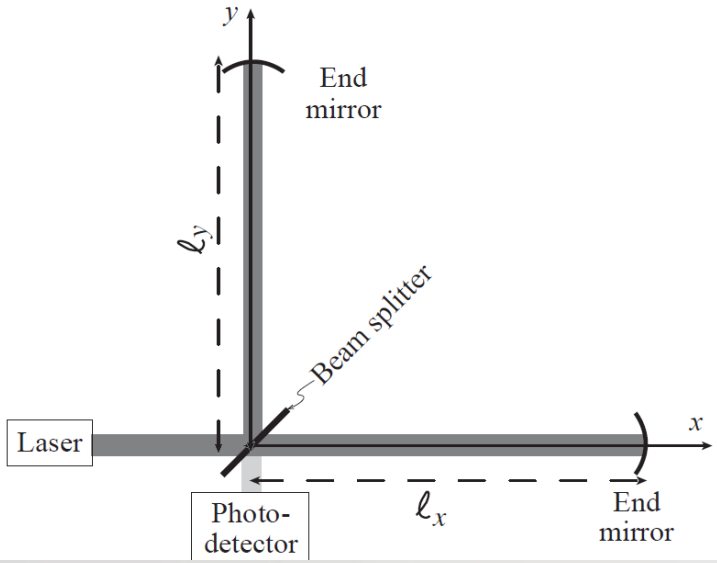

Laser Interferometer

- Gertsenstein, Pustovoit 1962

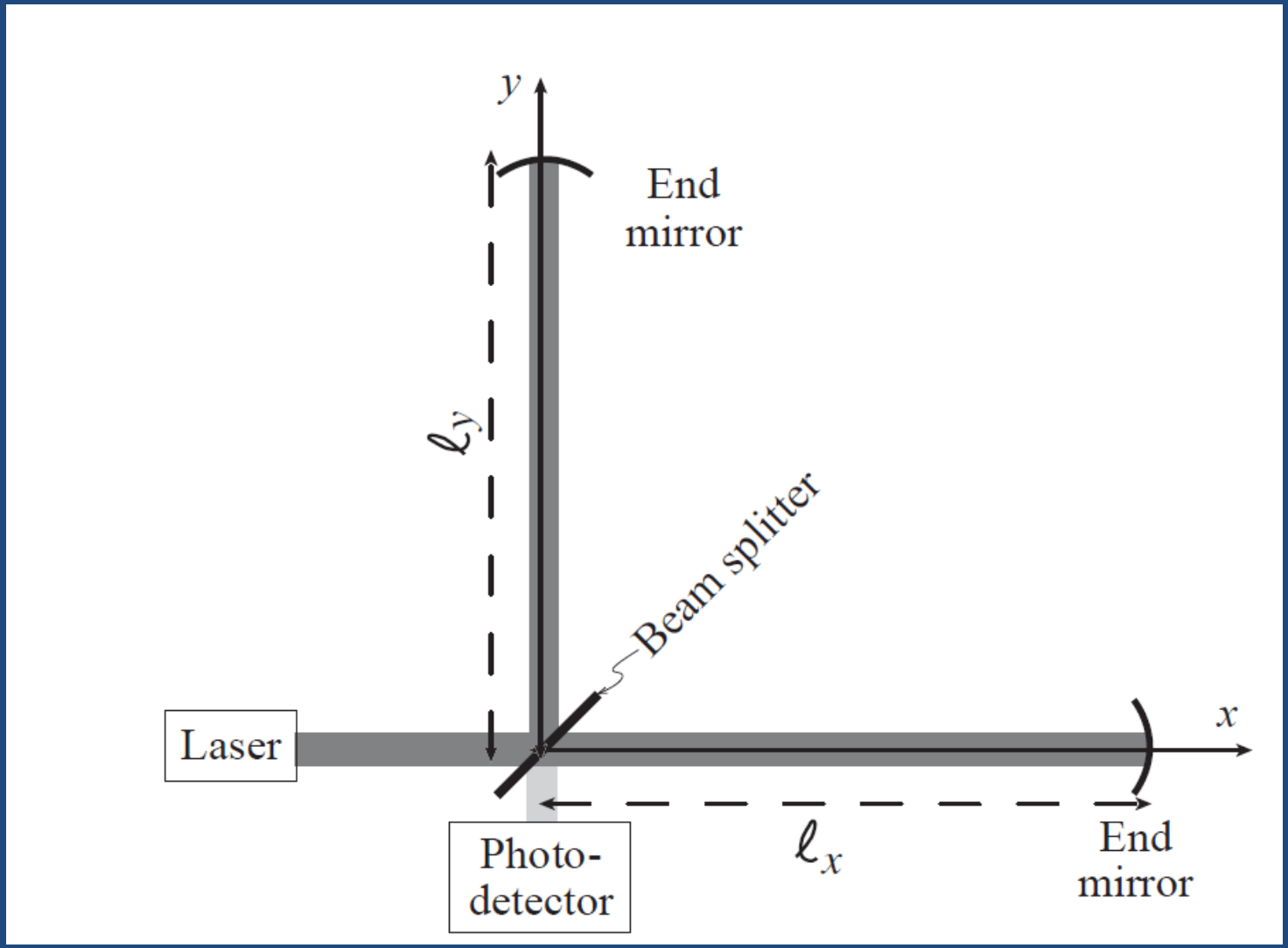

$$ds^2 = -dt^2 + [1 + h_+(t-z)]dx^2 + [1 - h_+(t-z)]dy^2 + dz^2$$

Principle of operation

$$\delta x = \frac{1}{2} h_+ \ell_x \qquad \delta y = -\frac{1}{2} h_+ \ell_y$$

Phase difference

$$\Delta\varphi(t) = \omega_o(2\delta y - 2\delta x) = \omega_o(\ell_x + \ell_y)h_+(t)$$

Intensity modulation

$$\Delta I_{\mathrm{PD}}(t) \propto \Delta\varphi(t) = 2\omega_o \ell h_+(t)$$

Achievable sensitivity

$$\Delta\Phi = B\frac{hL}{\lambda}, \quad \frac{BL}{c} \le \frac{1}{2}\left(\frac{1}{f_{GW}}\right) \Rightarrow B_{\max} \approx 400$$

$$Shot\ noise: \ \Delta\Phi_{\min} \sim \frac{1}{\sqrt{N_{ph}}},$$

$$N_{ph} = \frac{P_{laser} \times (\#\ recycling)}{\hbar\omega} \times \Delta t \sim 2\times 10^{20}$$

$$@\ P = 60W, \ \Delta t = 10ms$$

$$h_{\min} \sim \frac{\lambda}{BL}\frac{1}{\sqrt{N_{ph}}} = \frac{0.5\mu}{400\times 4km}\frac{1}{\sqrt{2\times 10^{20}}} \sim 10^{-22}\,!$$

LIGO interferometer

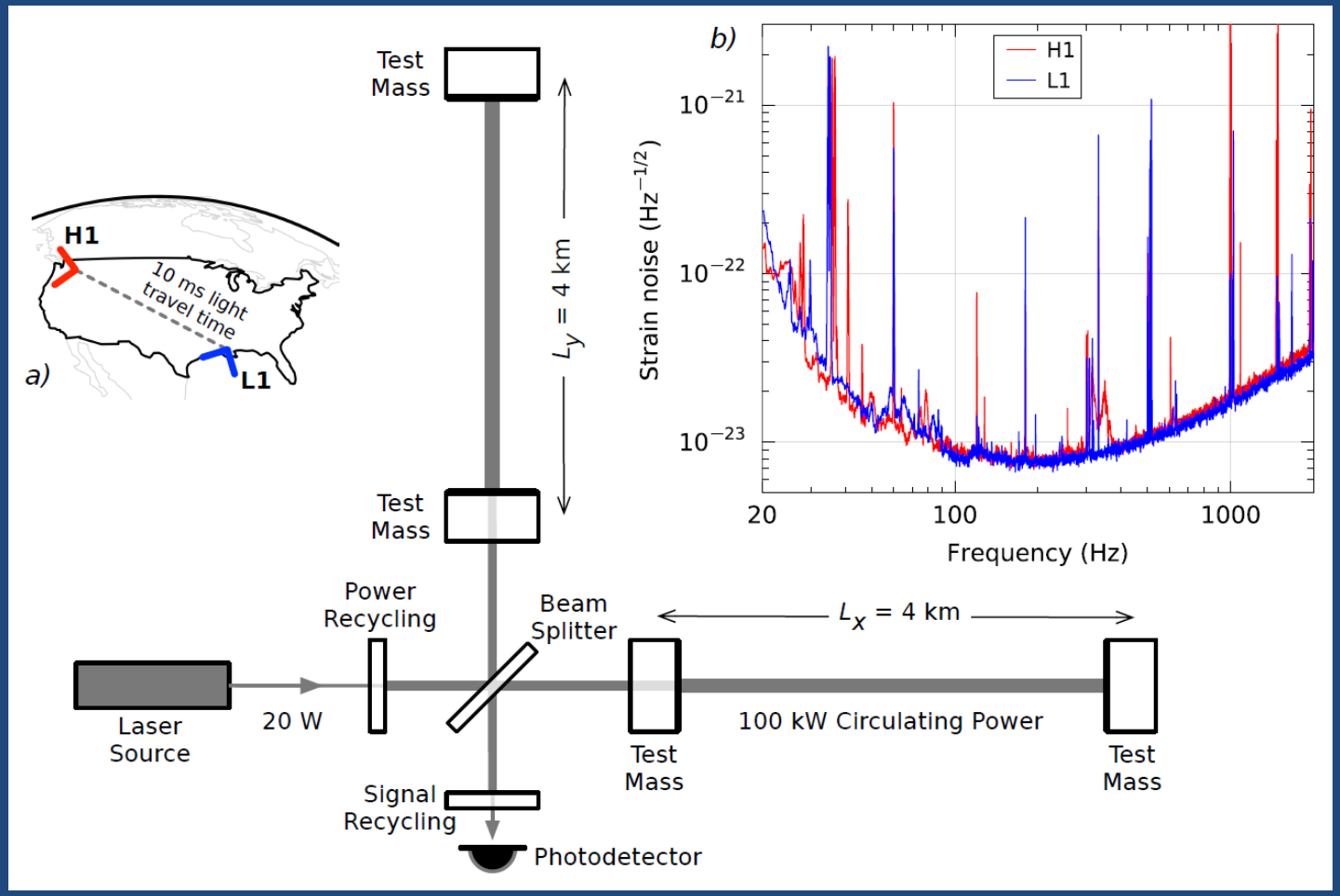

D. Reitze Phys.-Usp. 2017

Noise budget

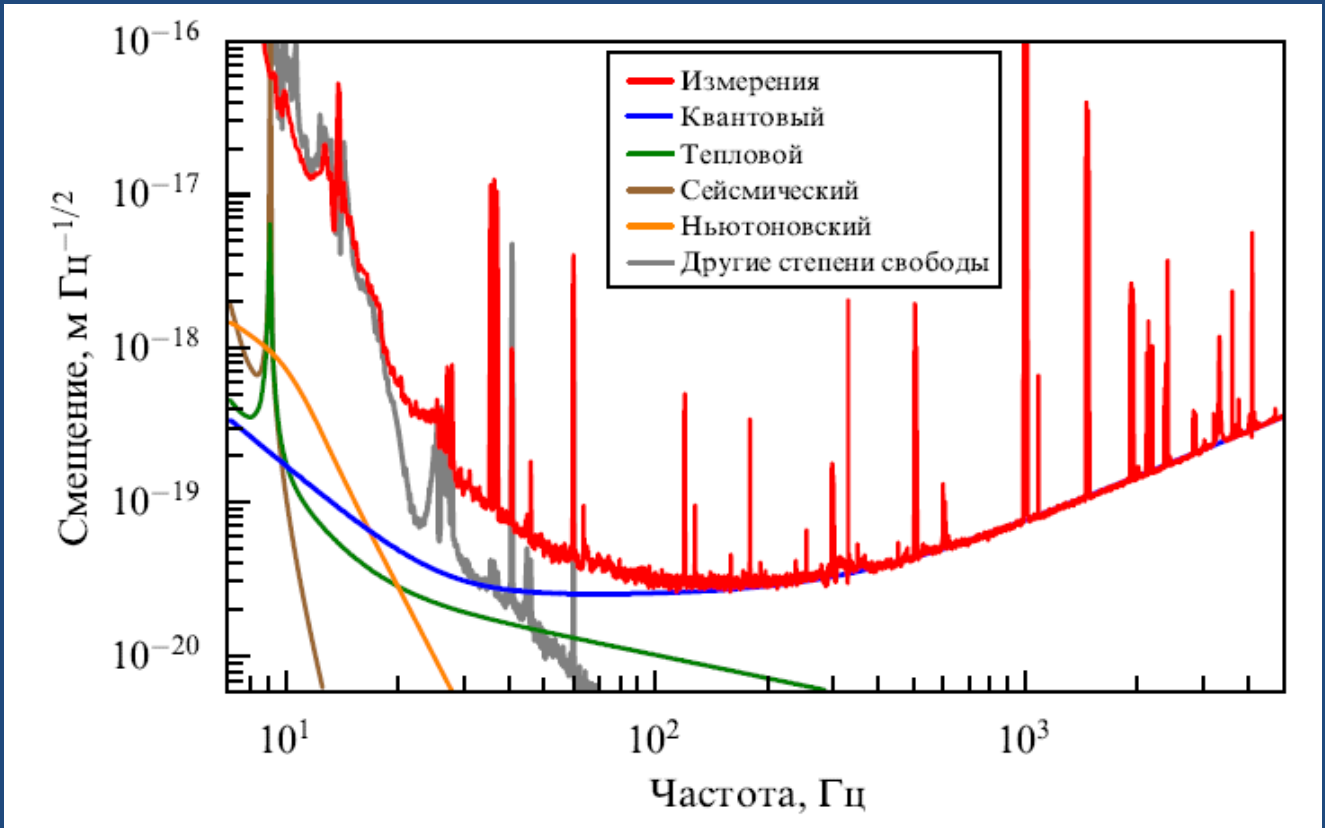

LIGO
Hanford
USA

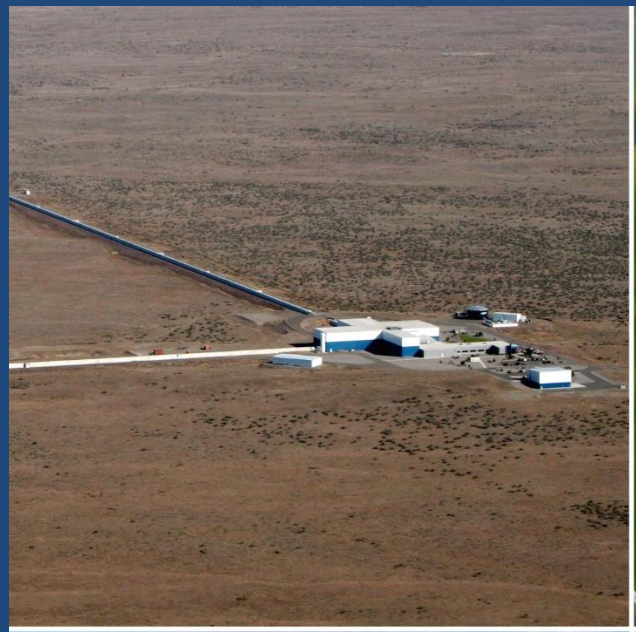

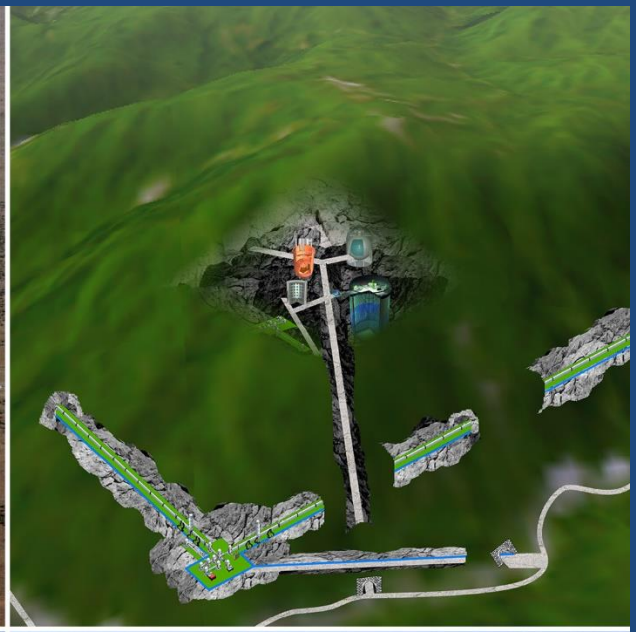

KAGRA
Kamioka
Japan

Virgo
Pisa
Italy

LIGO
Livingston
USA

Credit: LVC collab., Univ. of Tokyo

GW signal from first GW150914

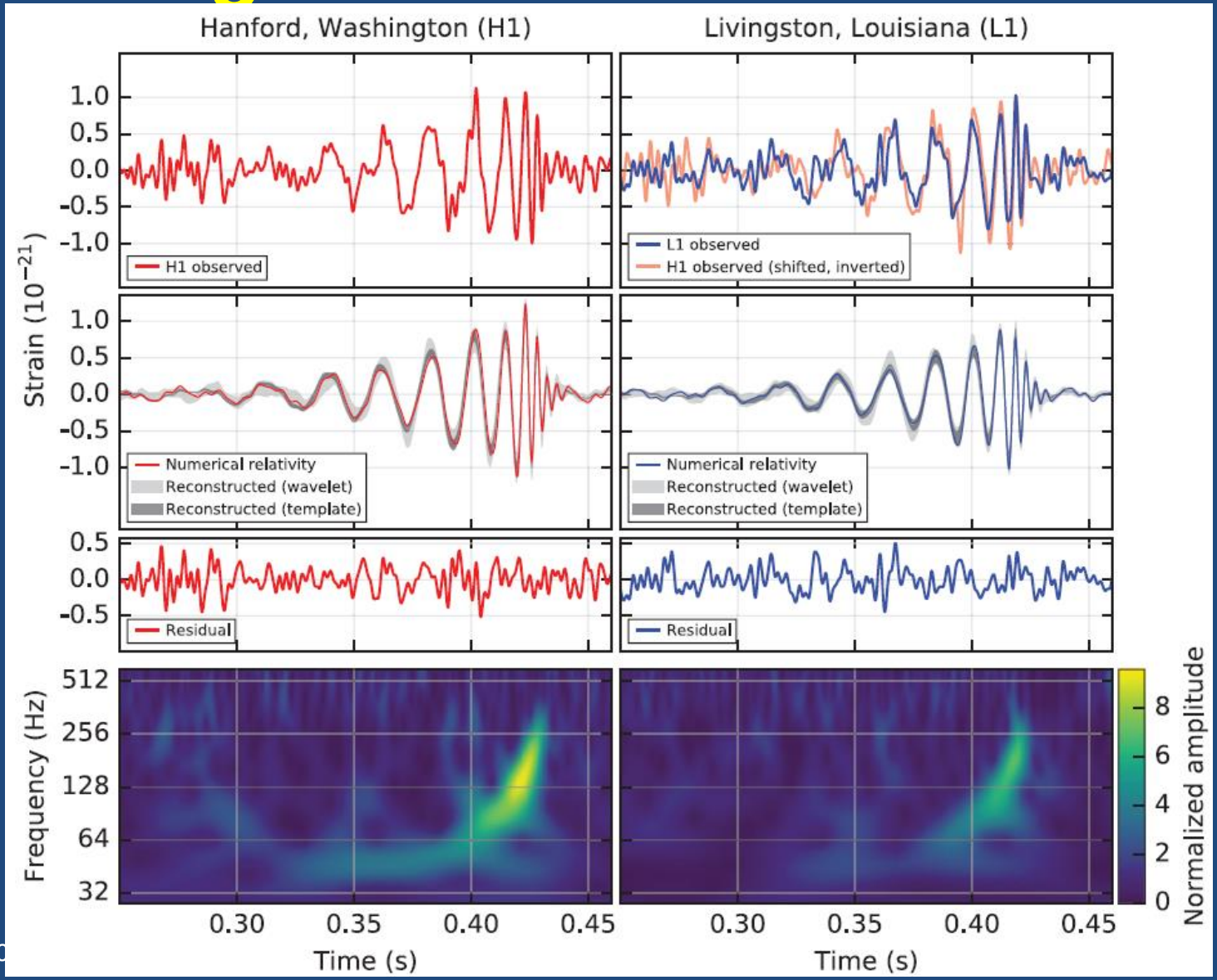

GW 150914 template vs observations: 94(+2/-3)%

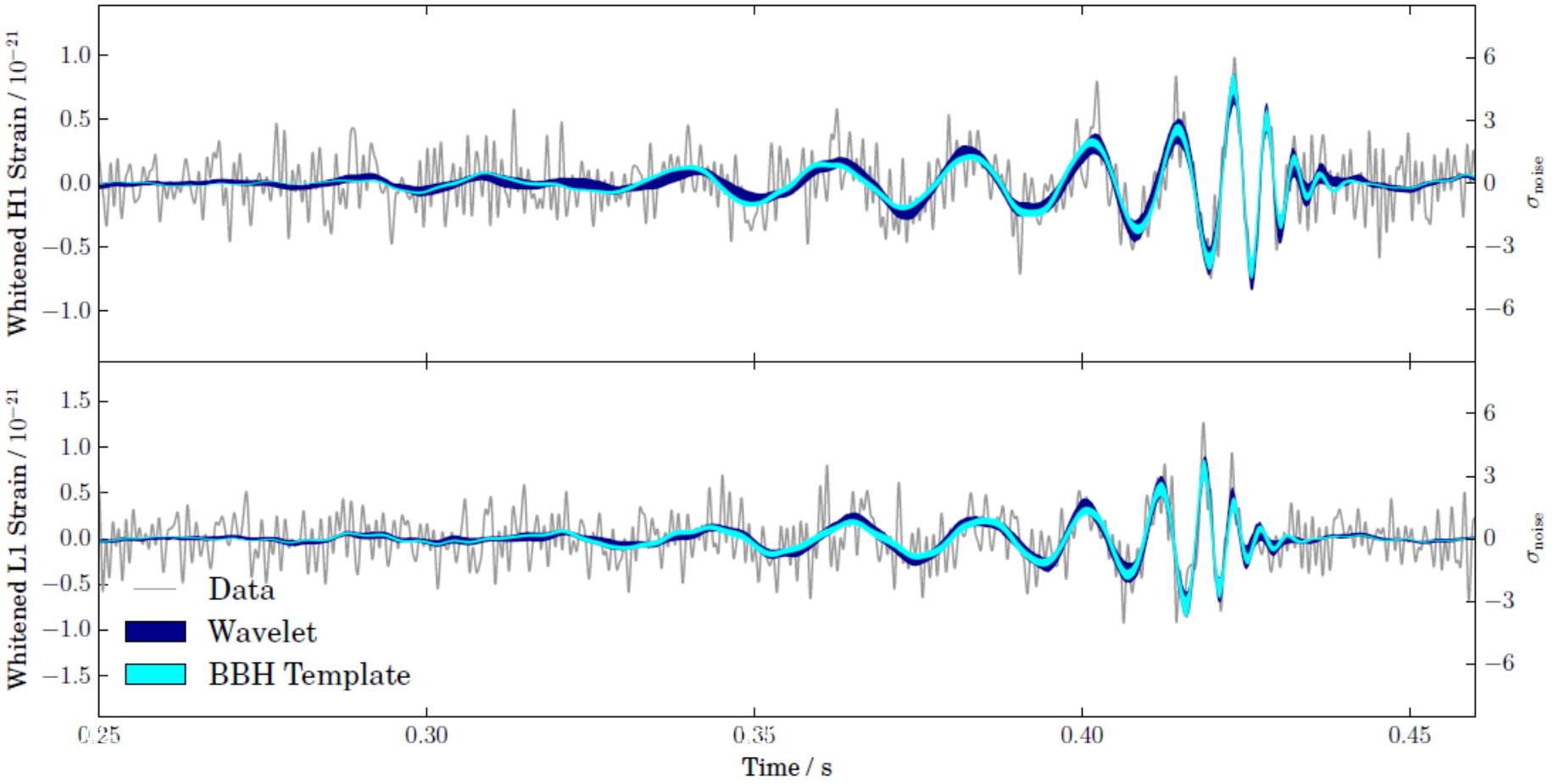

Principal sources: compact binary coalescences

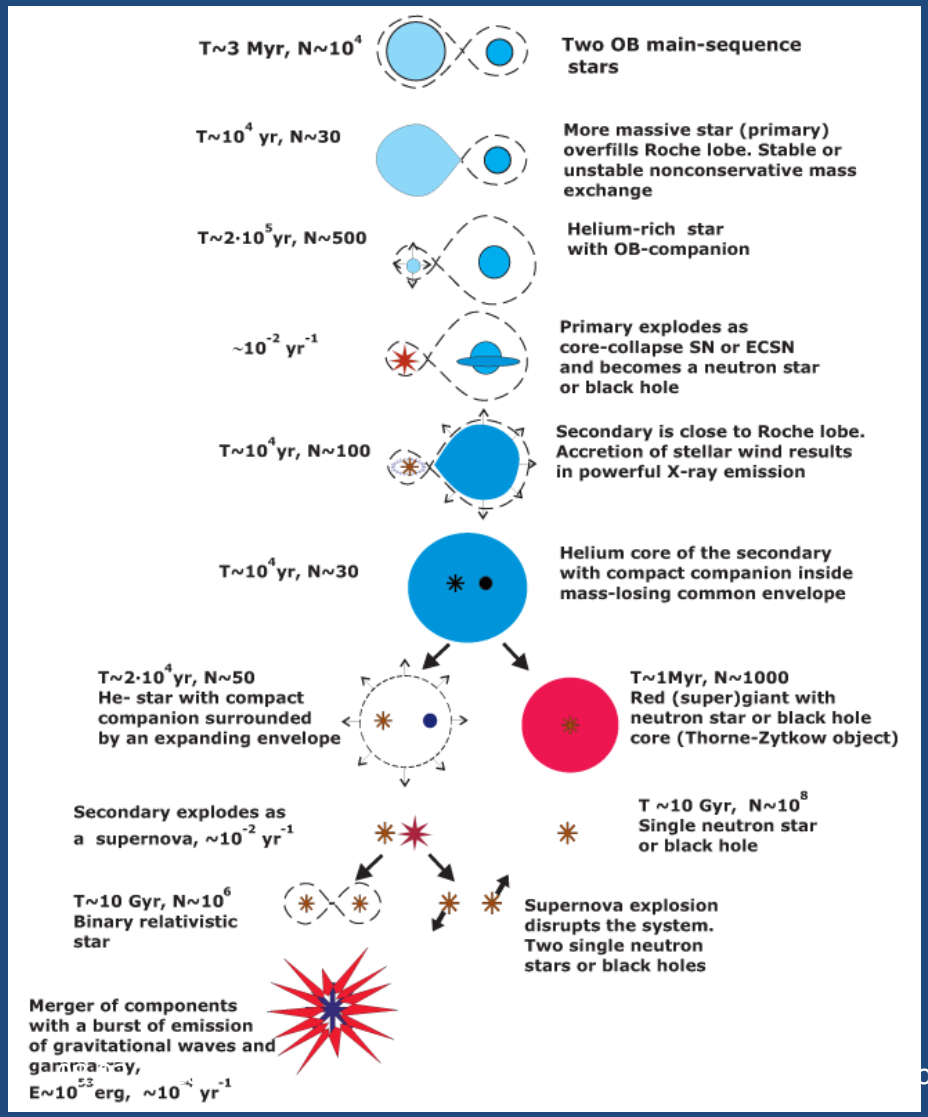

Evolution of massive binaries

Tutukov, Yungelson 1993
Lipunov, Postnov, Prokhorov 1997
.....

Other scenarios:

Dynamical interactions in stellar clusters

Exotica (primordial BHs)

...

Current status of GW interferometers

- O3 LIGO/Virgo/GEO-600 since April 2, 2019
- KAGRA underground GW interferometer started commissioning run on October 4, 2019

O3 Detection horizon

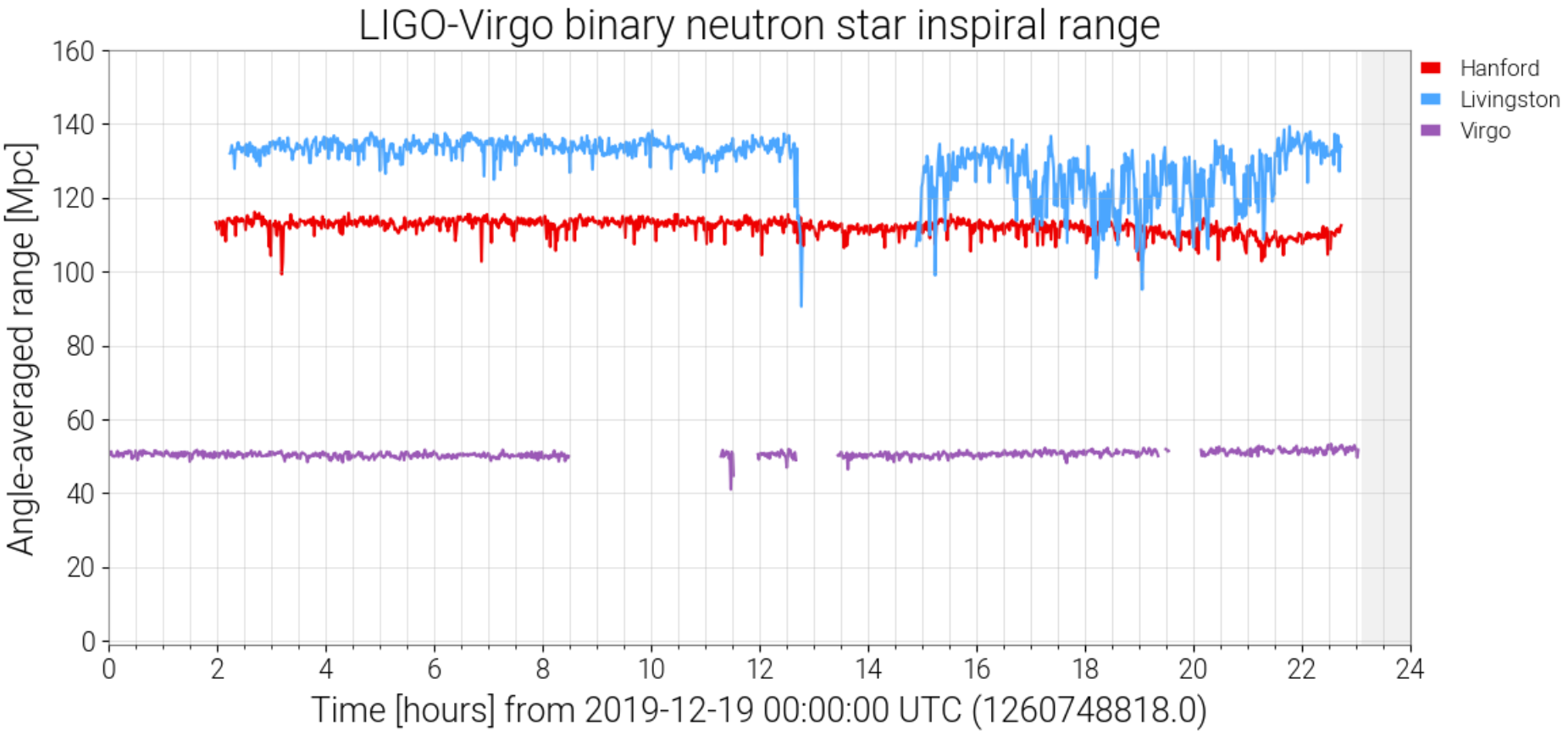

$D_h \sim M_{chirp}^{5/6}$

https://www.gw-openscience.org/

LVC O3 detections (as of 06.03.20)

54 triggers, 44 BH+BH, 5 NS+NS, 5 NS+BH candidates

https://gracedb.ligo.org

- No electromagnetic counterparts so far

Parameters from GW observations

$$\mathcal{M} = \frac{(m_1 m_2)^{3/5}}{M^{1/5}}$$

Chirp mass

$$\chi_{\rm eff} = \frac{(m_1 \vec{\chi}_1 + m_2 \vec{\chi}_2) \cdot \hat{L}_N}{M}$$

Effective spin

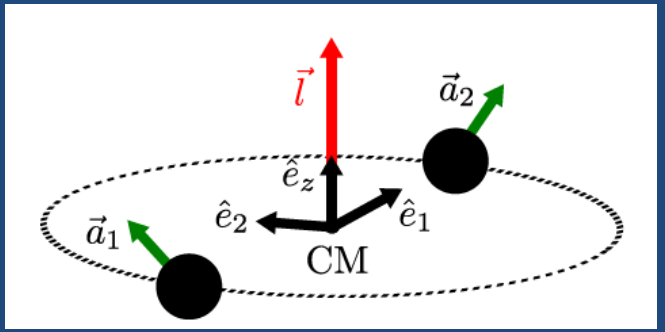

Event	$m_1/M_\odot$	$m_2/M_\odot$	$\mathcal{M}/M_\odot$	$\chi_{\rm eff}$	$M_{\rm f}/M_\odot$	$a_{\rm f}$	$E_{\rm rad}/(M_\odot c^2)$	$\ell_{\rm peak}/({\rm erg\,s^{-1}})$	$d_L/{\rm Mpc}$	z	$\Delta\Omega/{\rm deg}^2$
GW150914	$35.6^{+4.8}_{-3.0}$	$30.6^{+3.0}_{-4.4}$	$28.6^{+1.6}_{-1.5}$	$-0.01^{+0.12}_{-0.13}$	$63.1^{+3.3}_{-3.0}$	$0.69^{+0.05}_{-0.04}$	$3.1^{+0.4}_{-0.4}$	$3.6^{+0.4}_{-0.4}\times10^{56}$	430^{+150}_{-170}	$0.09^{+0.03}_{-0.03}$	180
GW151012	$23.3^{+14.0}_{-5.5}$	$13.6^{+4.1}_{-4.8}$	$15.2^{+2.0}_{-1.1}$	$0.04^{+0.28}_{-0.19}$	$35.7^{+9.9}_{-3.8}$	$0.67^{+0.13}_{-0.11}$	$1.5^{+0.5}_{-0.5}$	$3.2^{+0.8}_{-1.7}\times10^{56}$	1060^{+540}_{-480}	$0.21^{+0.09}_{-0.09}$	1555
GW151226	$13.7^{+8.8}_{-3.2}$	$7.7^{+2.2}_{-2.6}$	$8.9^{+0.3}_{-0.3}$	$0.18^{+0.20}_{-0.12}$	$20.5^{+6.4}_{-1.5}$	$0.74^{+0.07}_{-0.05}$	$1.0^{+0.1}_{-0.2}$	$3.4^{+0.7}_{-1.7}\times10^{56}$	440^{+180}_{-190}	$0.09^{+0.04}_{-0.04}$	1033
GW170104	$31.0^{+7.2}_{-5.6}$	$20.1^{+4.9}_{-4.5}$	$21.5^{+2.1}_{-1.7}$	$-0.04^{+0.17}_{-0.20}$	$49.1^{+5.2}_{-3.9}$	$0.66^{+0.08}_{-0.10}$	$2.2^{+0.5}_{-0.5}$	$3.3^{+0.6}_{-0.9}\times10^{56}$	960^{+430}_{-410}	$0.19^{+0.07}_{-0.08}$	924
GW170608	$10.9^{+5.3}_{-1.7}$	$7.6^{+1.3}_{-2.1}$	$7.9^{+0.2}_{-0.2}$	$0.03^{+0.19}_{-0.07}$	$17.8^{+3.2}_{-0.7}$	$0.69^{+0.04}_{-0.04}$	$0.9^{+0.05}_{-0.1}$	$3.5^{+0.4}_{-1.3}\times10^{56}$	320^{+120}_{-110}	$0.07^{+0.02}_{-0.02}$	396
GW170729	$50.6^{+16.6}_{-10.2}$	$34.3^{+9.1}_{-10.1}$	$35.7^{+6.5}_{-4.7}$	$0.36^{+0.21}_{-0.25}$	$80.3^{+14.6}_{-10.2}$	$0.81^{+0.07}_{-0.13}$	$4.8^{+1.7}_{-1.7}$	$4.2^{+0.9}_{-1.5}\times10^{56}$	2750^{+1350}_{-1320}	$0.48^{+0.19}_{-0.20}$	1033
GW170809	$35.2^{+8.3}_{-6.0}$	$23.8^{+5.2}_{-5.1}$	$25.0^{+2.1}_{-1.6}$	$0.07^{+0.16}_{-0.16}$	$56.4^{+5.2}_{-3.7}$	$0.70^{+0.08}_{-0.09}$	$2.7^{+0.6}_{-0.6}$	$3.5^{+0.6}_{-0.9}\times10^{56}$	990^{+320}_{-380}	$0.20^{+0.05}_{-0.07}$	340
GW170814	$30.7^{+5.7}_{-3.0}$	$25.3^{+2.9}_{-4.1}$	$24.2^{+1.4}_{-1.1}$	$0.07^{+0.12}_{-0.11}$	$53.4^{+3.2}_{-2.4}$	$0.72^{+0.07}_{-0.05}$	$2.7^{+0.4}_{-0.3}$	$3.7^{+0.4}_{-0.5}\times10^{56}$	580^{+160}_{-210}	$0.12^{+0.03}_{-0.04}$	87
GW170817	$1.46^{+0.12}_{-0.10}$	$1.27^{+0.09}_{-0.09}$	$1.186^{+0.001}_{-0.001}$	$0.00^{+0.02}_{-0.01}$	≤ 2.8	≤ 0.89	≥ 0.04	$\geq 0.1\times10^{56}$	40^{+10}_{-10}	$0.01^{+0.00}_{-0.00}$	16
GW170818	$35.5^{+7.5}_{-4.7}$	$26.8^{+4.3}_{-5.2}$	$26.7^{+2.1}_{-1.7}$	$-0.09^{+0.18}_{-0.21}$	$59.8^{+4.8}_{-3.8}$	$0.67^{+0.07}_{-0.08}$	$2.7^{+0.5}_{-0.5}$	$3.4^{+0.5}_{-0.7}\times10^{56}$	1020^{+430}_{-360}	$0.20^{+0.07}_{-0.07}$	39
GW170823	$39.6^{+10.0}_{-6.6}$	$29.4^{+6.3}_{-7.1}$	$29.3^{+4.2}_{-3.2}$	$0.08^{+0.20}_{-0.22}$	$65.6^{+9.4}_{-6.6}$	$0.71^{+0.08}_{-0.10}$	$3.3^{+0.9}_{-0.8}$	$3.6^{+0.6}_{-0.9}\times10^{56}$	1850^{+840}_{-840}	$0.34^{+0.13}_{-0.14}$	1651

LIGO BH: Masses

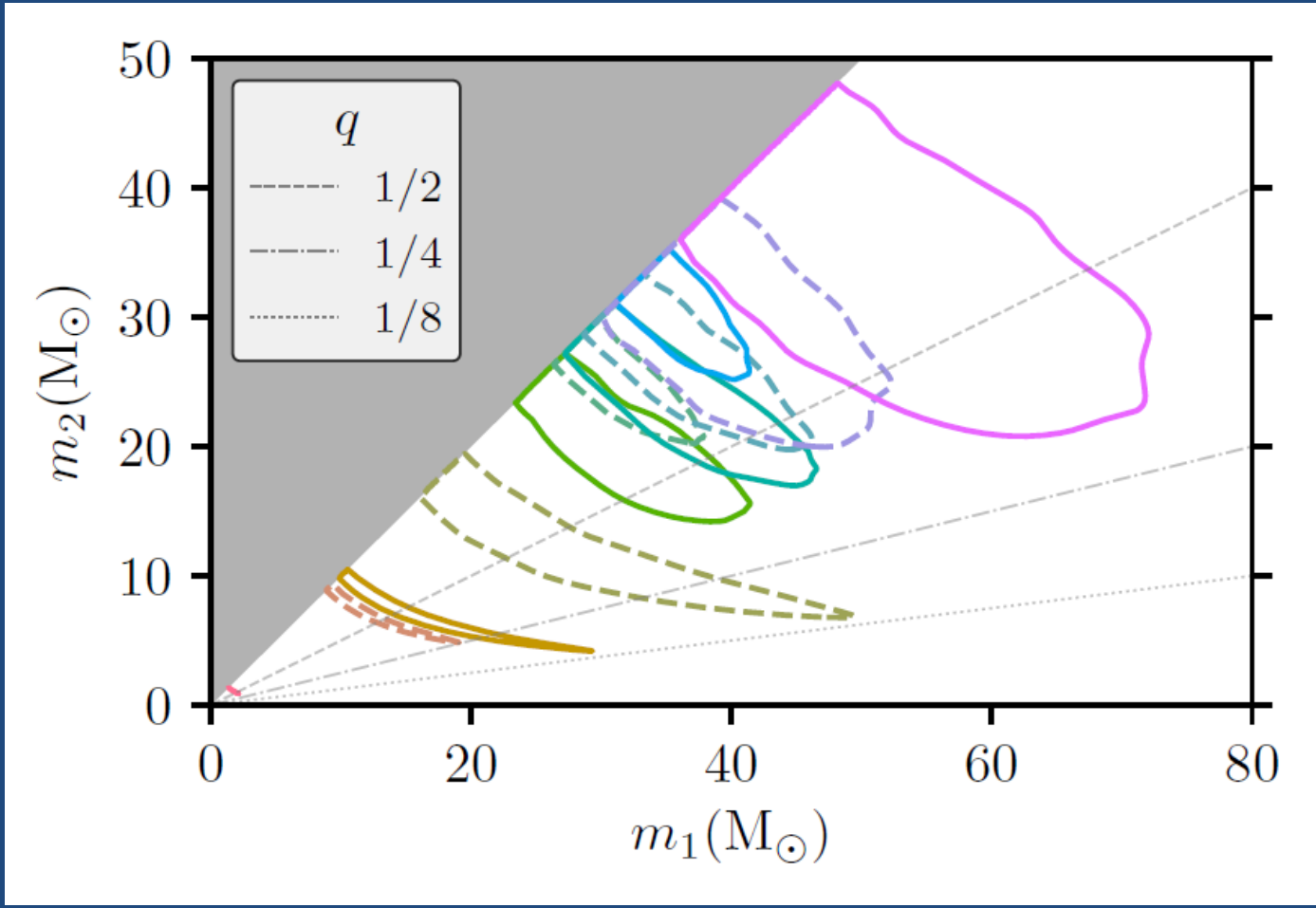

LIGO BH: effective spins consistent with zero

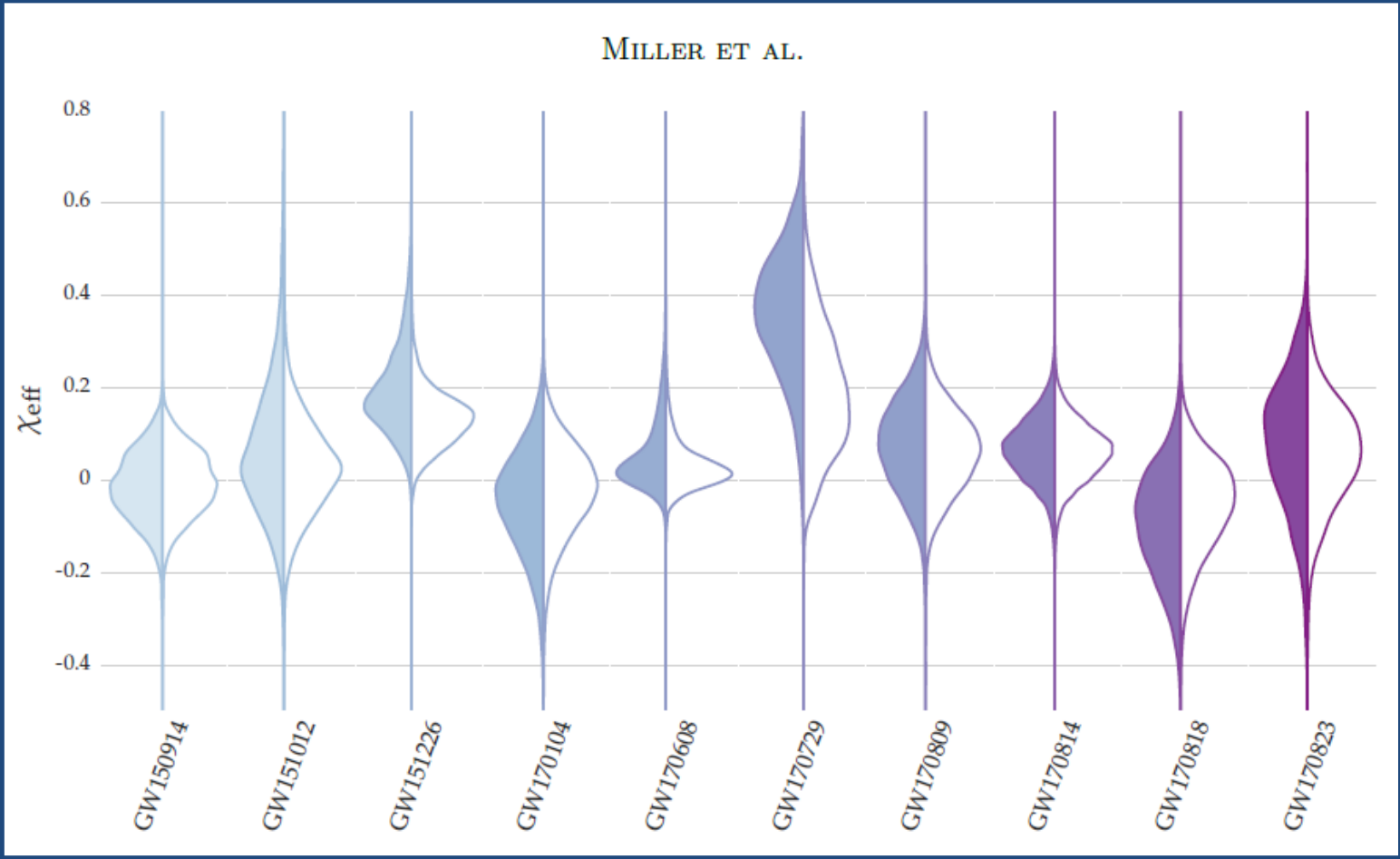

Corollary:

- Larger masses (compared to BHs in XRBs)
- Low effective spins (but possibly GW151226)

Predictions and surprises

- Binary BH+BH coalescences must be much more numerous and should be detected first (Tutukov, Yungelson 1993, Lipunov, Postnov, Prokhorov 1997,….confirmed!)
- Mass of BH in LIGO binaries is up to ~50 M$\odot$ (surprise, but can be reconciled with stellar evolution)
- Low effective spins (surprise, but can be reconciled with binary evolution) (PK+'19, Fuller+19…)

BH+BH mass and spin distributions before coalescence

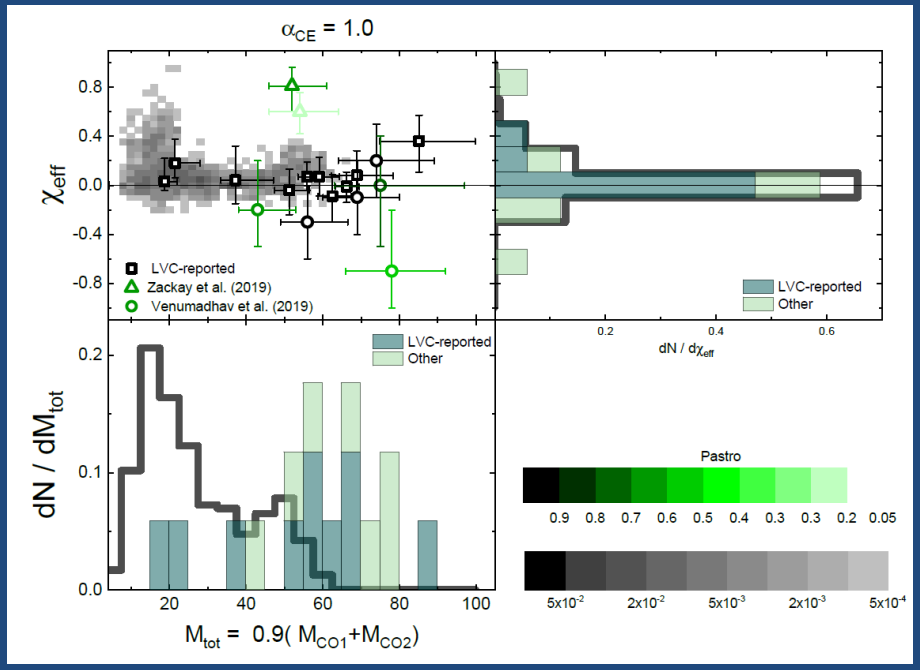

Without fallback

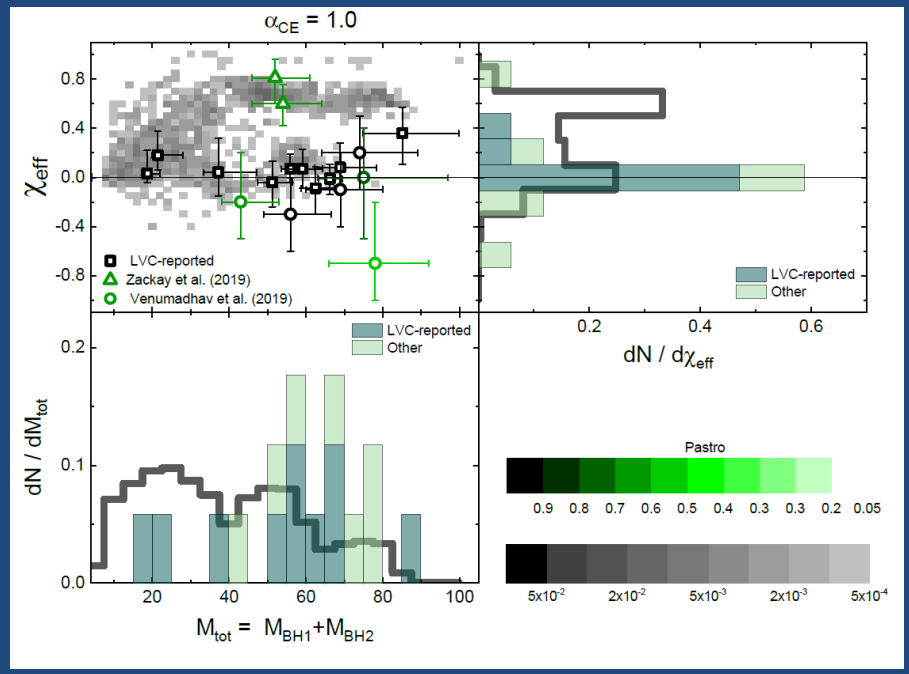

+ fallback from envelope

PK+ 2019, Physics-Uspekhi (2019, No 11, in press)

MNRAS **483**, 3288–3306 (2019)

Table 2. Candidate events in the full search of O1 and O2 data. Candidates are sorted by FAR evaluated for the entire b
of templates. Note that ranking statistic and false alarm rate may not have a strictly monotonic relationship due to var
data quality between sub-analyses. The mass and spin parameters listed are associated with the template waveform yiel
the highest ranked multi-detector event for each candidate, and may differ significantly from full Bayesian parameter estima
Masses are quoted in detector frame, and are thus larger than source frame masses by a factor $(1+z)$, where z is the so
redshift.

Date designation	GPS time	FAR^{-1} (y)	Detectors	$\tilde{\Lambda}$	ρ_H	ρ_L	ρ_V	m_1	m_2	$\chi_{\rm eff}$
170817+12:41:04UTC	1187008882.45	> 10000	HL	180.46	18.6	24.3	-	1.5	1.3	-0.00
150914+09:50:45UTC	1126259462.43	> 10000	HL	93.82	19.7	13.4	-	44.2	32.2	0.09
170104+10:11:58UTC	1167559936.60	> 10000	HL	35.54	9.0	9.6	-	47.9	16.0	0.03
170823+13:13:58UTC	1187529256.52	> 10000	HL	55.04	6.3	9.2	-	68.9	47.2	0.23
170814+10:30:43UTC	1186741861.54	> 10000	HL	52.85	9.0	13.0	-	58.7	23.3	0.53
151226+03:38:53UTC	1135136350.65	> 10000	HL	42.90	10.7	7.4	-	14.8	8.5	0.24
170809+08:28:21UTC	1186302519.76	9400	HL	40.59	6.6	10.7	-	36.0	33.7	0.07
170608+02:01:16UTC	1180922494.49	> 910[a]	HL	51.01	12.5	8.7	-	16.8	6.1	0.31
151012+09:54:43UTC	1128678900.45	220	HL	20.18	7.0	6.7	-	30.8	12.9	-0.05
170729+18:56:29UTC	1185389807.33	6.4	HL	15.33	7.4	6.7	-	106.5	49.7	0.59
170121+21:25:36UTC	1169069154.58	1.3	HL	15.76	5.1	8.7	-	40.4	13.6	-0.98
170727+01:04:30UTC	1185152688.03	.53	HL	13.75	4.5	6.9	-	65.2	26.5	-0.35
170818+02:25:09UTC	1187058327.09	.22	HL	13.29	4.4	9.4	-	53.7	27.4	0.07
170722+08:45:14UTC	1184748332.91	.11	HL	12.19	5.0	6.4	-	248.1	7.1	0.99
170321+03:13:21UTC	1174101219.23	.1	HL	12.22	6.5	6.4	-	11.0	1.3	-0.89
170310+09:30:52UTC	1173173470.77	.07	HL	12.15	6.1	6.2	-	2.1	1.1	-0.20
170809+03:55:52UTC	1186286170.08	.07	LV	7.34	-	7.0	5.1	6.2	1.2	0.60
170819+07:30:53UTC	1187163071.23	.05	HV	11.35	6.3	-	6.7	135.2	2.5	0.85
170618+20:00:39UTC	1181851257.72	.05	HL	11.49	5.2	6.7	-	2.9	2.1	0.30
170416+18:38:48UTC	1176403146.15	.04	HL	11.21	5.1	6.9	-	7.8	1.1	-0.47
170331+07:08:18UTC	1174979316.31	.04	HL	11.03	5.2	7.0	-	3.9	1.1	-0.34
151216+18:49:30UTC	1134326987.60	.04	HL	11.54	6.1	6.0	-	13.9	5.0	-0.41
170306+04:45:50UTC	1172810768.08	.04	HL	11.47	4.8	7.3	-	26.4	1.8	0.23
151227+16:52:22UTC	1135270359.27	.04	HL	11.75	7.3	4.6	-	154.5	4.9	1.00
170126+23:56:22UTC	1169510200.17	.04	HL	11.61	6.4	5.7	-	4.9	1.3	0.79
151202+01:18:13UTC	1133054310.55	.03	HL	11.48	6.5	5.7	-	40.4	1.8	-0.26
170208+20:23:00UTC	1170620598.15	.03	HL	11.12	6.8	5.4	-	6.9	1.0	0.09
170327+17:07:35UTC	1174669673.72	.03	HL	10.65	6.0	6.2	-	40.1	1.0	0.97
170823+13:40:55UTC	1187530873.86	.03	LV	9.30	-	8.0	5.8	117.9	1.3	0.98
150928+10:49:00UTC	1127472557.93	.03	HL	11.28	6.0	6.3	-	2.5	1.0	-0.70

New candidates from O1 and O2

1910.05331

Independent detections: a new trend?

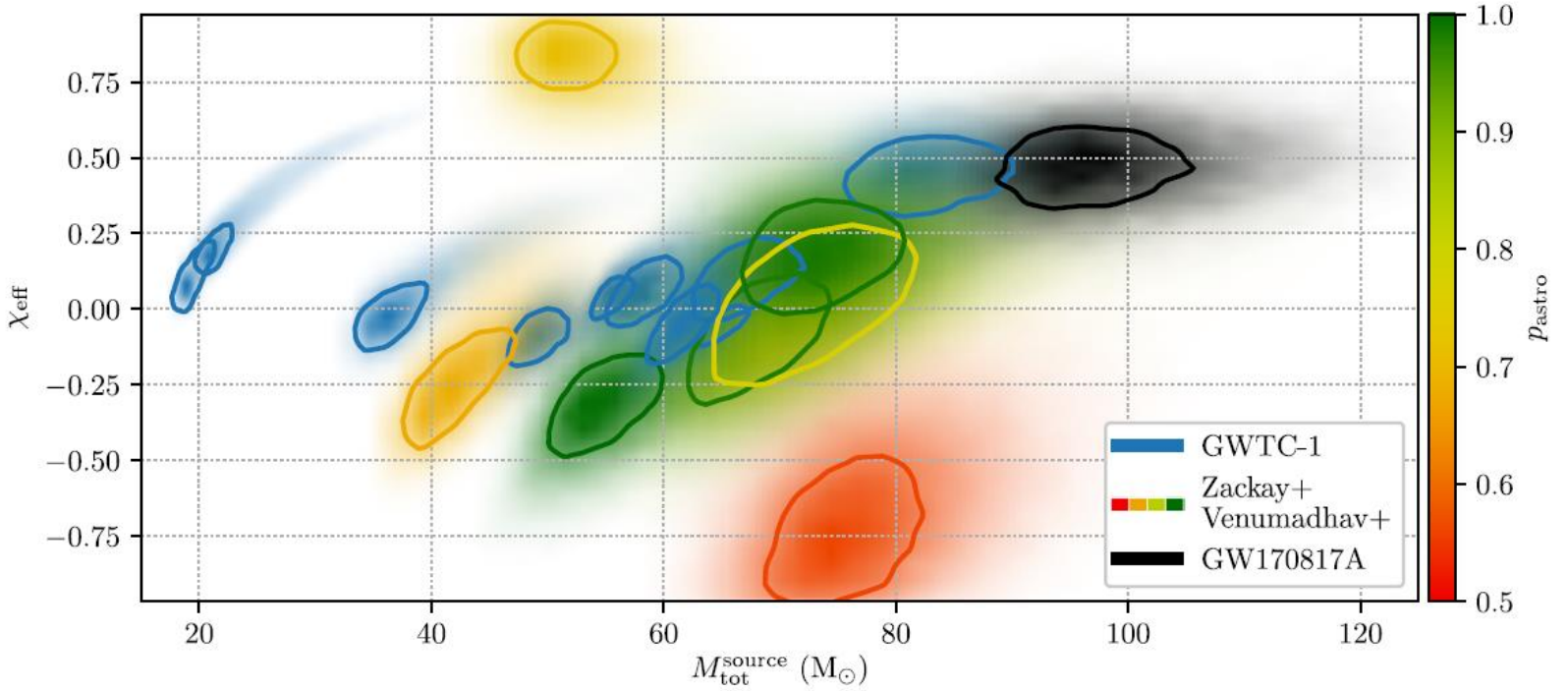

FIG. 7: Binary black holes events reported from O1 and O2, in the plane of source-frame total mass vs. effective spin. In blue are shown the 10 BBH events reported in GWTC-1 [1], all of them are certainly astrophysical in origin ($p_{\rm astro} = 1$). Color coded by $p_{\rm astro}$ are shown 7 additional events with $p_{\rm astro} > 0.5$ that our previous searches found [2, 4]. In black we show GW170817A. Displayed are 1σ probability contours, i.e. enclosing $1 - e^{-1/2} \approx 0.39$ of the probability distribution.

1910.09528

Massive BH+BH: New physics ?

- Stellar-mass primordial black holes:
  - Can be formed in the early Universe in different models (Carr, Hawking'74)
  - Can be in binaries (Nakamura+'97)
  - Can naturally explain low spins of observed BH+BH (Bird+'16, Blinnikov+'16,…)
  - Can substantially contribute to dark matter
  - Can be seeds for growth of SMBH in galactic centers

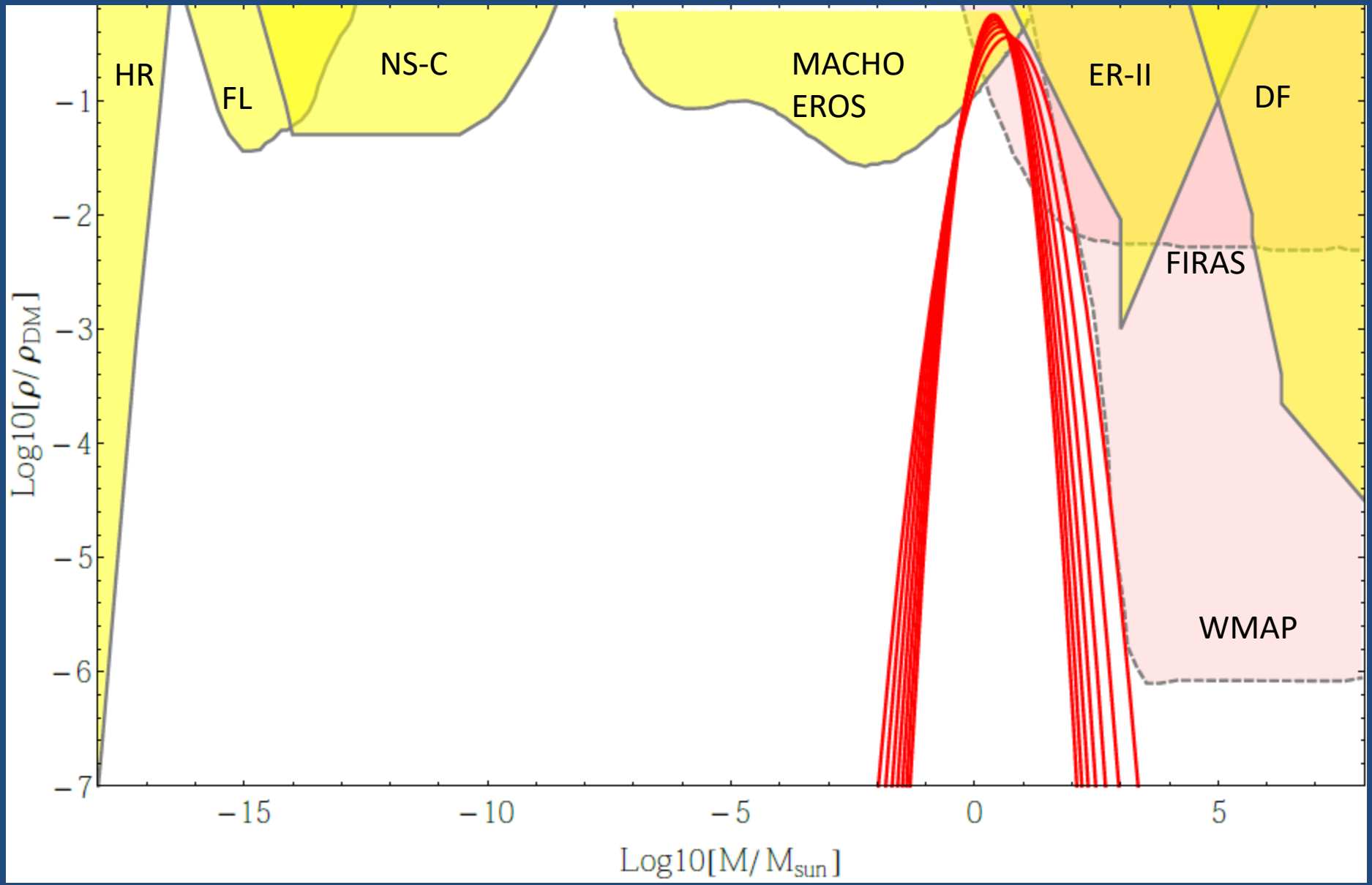

Blinnikov, Dolgov, PK, Porayko 2016 JCAP 11 036

Present constraints (model-dependent)

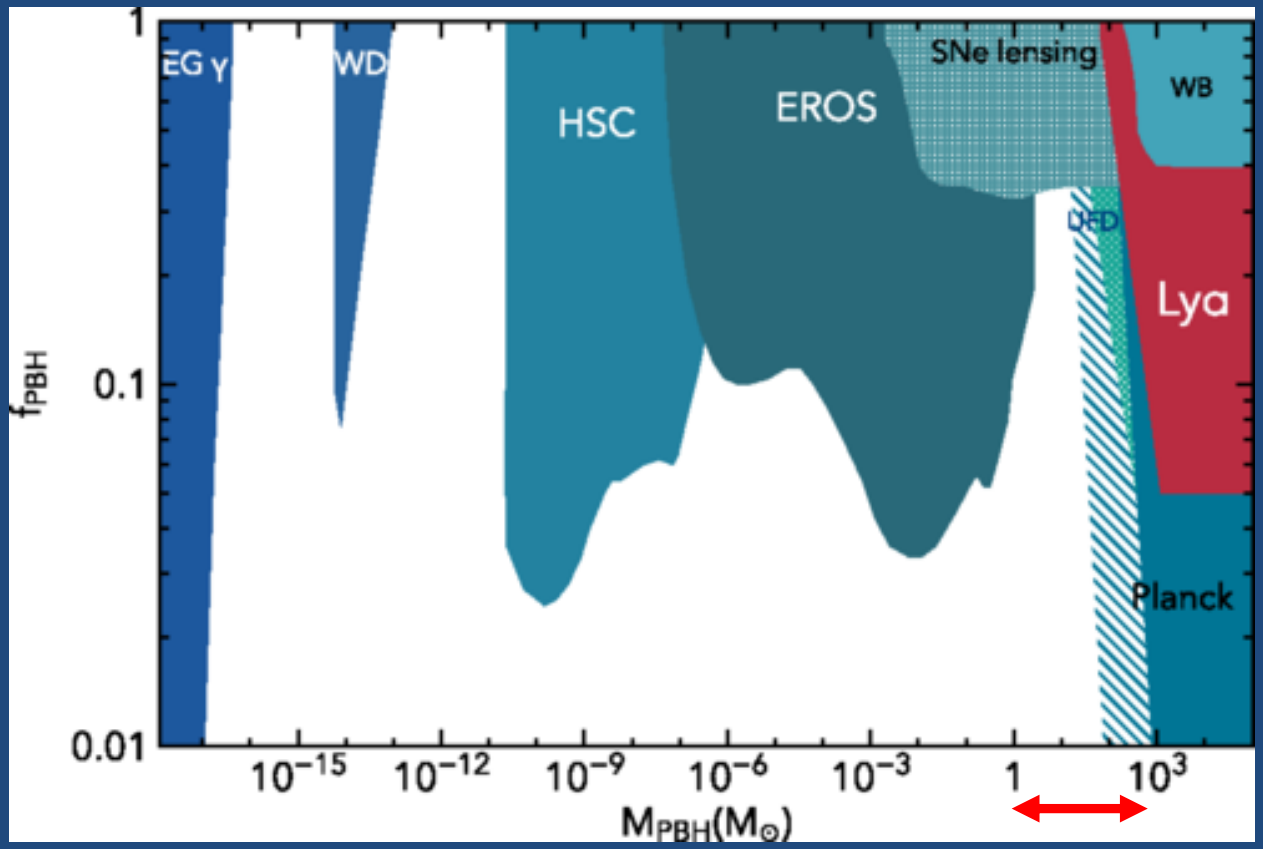

1-100 M⊙ PBH are still in the open window!

Murgia+'19

GW road map (official)

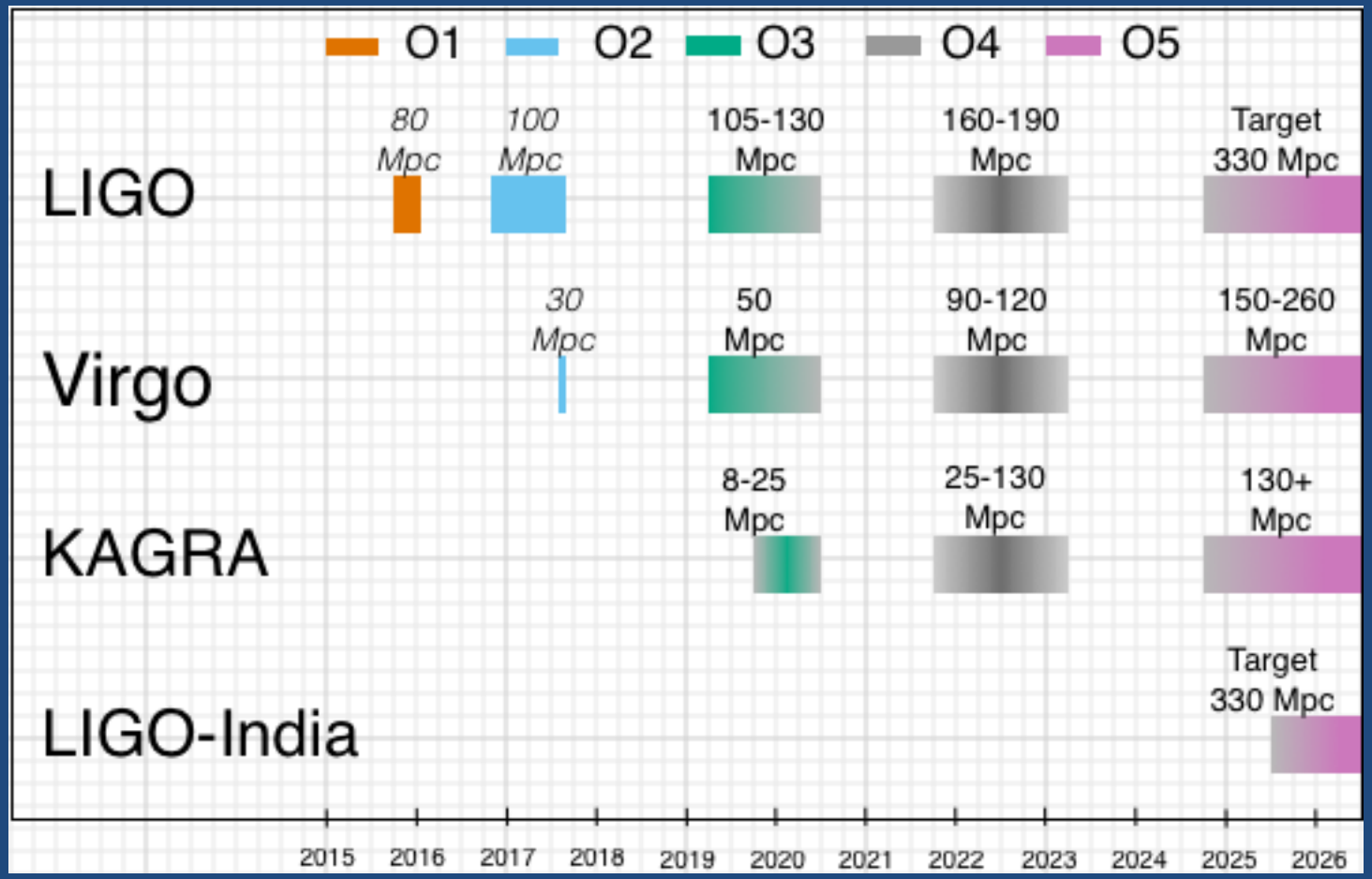

40-км LIGO Cosmic Explorer (2035)

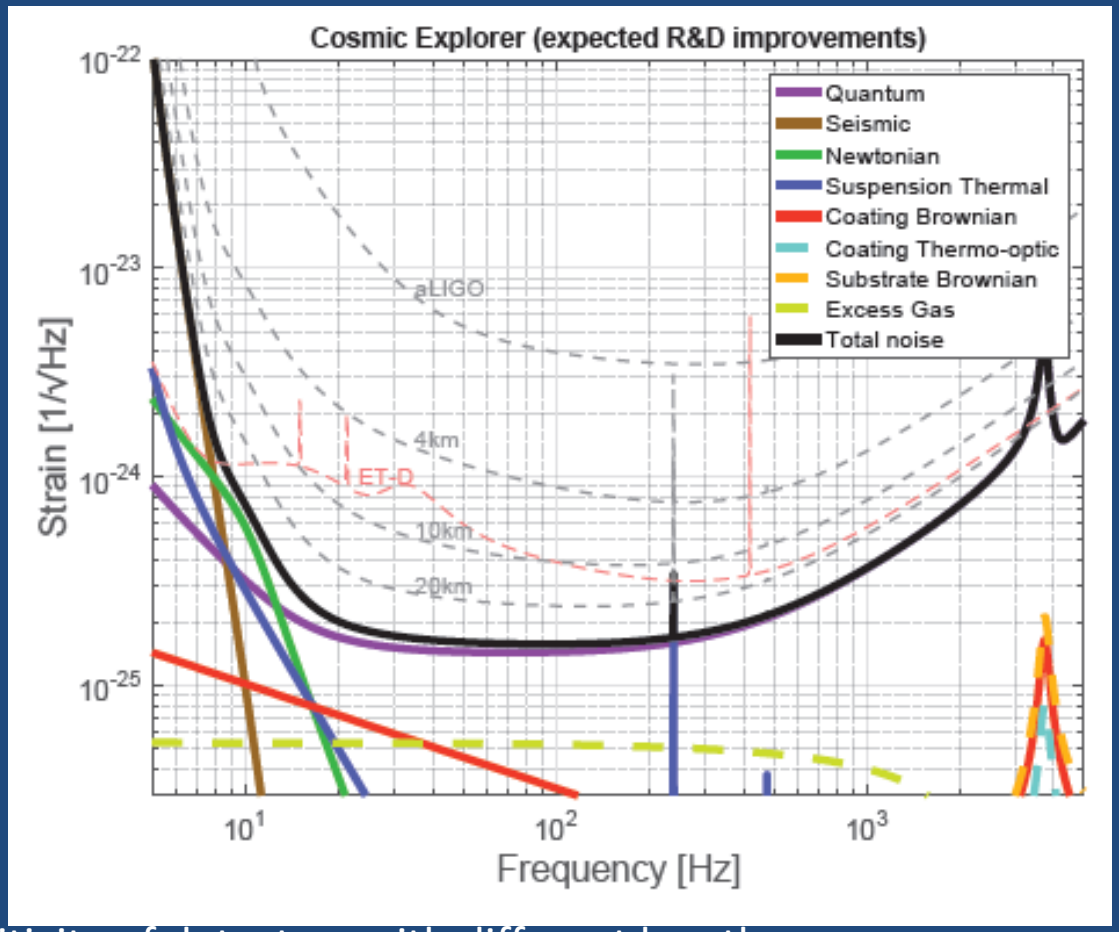

Sensitivity of detectors with different lengths.
Solid curves are for a 40km long detector

LIGO Scientific Collaboration,arXiv:1607.08697 [astro-ph.IM]

Main results

- Binary blacl hpoles are main souerces in current LIGO/Virgo detections. Masses up to 50 solar masses. No deviations from GR.
- Merging rate in agreement with standard astrophysical predictions
- Effective spins are consistemt with zero
- Primordial BHs are still not excluded
- Increase in detector sensitivity is needed to probe GR at level better than 1%